1955

Passage of free electrons through ceramic materials

Roger Emerson Nolte
Iowa State College

PASSAGE OF FREE ELECTRONS THROUGH CERAMIC MATERIALS

by

Roger Emerson Nolte

A Dissertation Submitted to the

Graduate Faculty in Partial Fulfillment of

The Requirements for the Degree of

DOCTOR OF PHILOSOPHY

Major Subject: Electrical Engineering

Approved:

Signature was redacted for privacy.

In Charge of Major Work

Signature was redacted for privacy.

Head of Major Department

Signature was redacted for privacy.

Dean of Graduate College

Iowa State College

1955

TABLE OF CONTENTS

I. INTRODUCTION

A. Vacuum Tube Developments

The rapid growth of the electronic industry, with its many branches and specializations, has produced a tremendous number of different vacuum tubes and an even greater variety of applications. Military applications and requirements have accelerated developments in the vacuum tube industry and also act as a paramount challenge to tube performance and reliability.

The industry accepted this challenge by individually and collectively organizing tube reliability programs. These continuing programs are creating many redesigned versions of standard type tubes which have special designations and are more expensive than their mass-produced prototypes. At present most "reliable tube" programs consist of improving the mechanical supports and tolerances, during the construction phase, followed by elaborate aging cycles.

The resulting "reliable tubes" have a longer life expectancy than the standard product, which greatly increases the expected period of satisfactory operation of a complicated electronic system. For example, the performance of two tube groups will be compared in a 100 tube guided missile system. Under certain operating conditions for a period of 100 hours, assume four out of 100 standard tubes fail while one out of 100

"reliable tubes" fail. This represents per tube performance probabilities of 0.96 and 0.99 respectively. Assuming that the system fails when a tube fails, the system probabilities will be $(.96)^{100}$ (approximately 0.017) and $(.99)^{100}$ (approximately 0.36). This means that only 1.7 out of 100 standard tube systems can be expected to work for 100 hours compared to 36 out of 100 for the "reliable tube" systems. This example emphasizes the importance of continuing the reliability programs. Working a somewhat similar problem in reverse, a 400 tube missile with an 80 per cent success probability requires that on the average no more than one tube of 1800 fail in the specified length of time.

Although component parts of a system other than vacuum tubes fail and create reliability problems, in most systems tubes are considered responsible for over 50 per cent of system troubles. Studies by Acheson and McElwee (1) reveal that about 85 per cent of these tube troubles are in the form of changing characteristics or complete failure caused mostly by filament failure and movement of internal elements of the tube. This motion may be vibrational or it may be caused by faulty or shrinking spacers. Palmer (26) described a recent development using ceramic alumina for the spacers. The ceramic has excellent temperature characteristics, outgasses readily, and is superior to mica because of closer tolerances and better mechanical stability.

Tube reliability programs using tubes of conventional design are advancing in a somewhat asymptotic manner. It has been expressed that some new approaches to vacuum tube design are essential for continuing

progress. This dissertation represents such an approach: the use of a ceramic, permeable to free electrons, as a possible filler for an electronic tube.

The major part of this research deals with the basic problems of electron passage through different ceramic samples under various operating conditions. In Section IV, possible applications and future research are indicated and discussed.

B. The Problem

Because of its uniqueness, this investigation concerning the permeability of ceramics to free electrons under the influence of electric fields requires further introduction. The objective of this research is to introduce theories and experimental evidence that will initiate a better understanding of this phenomenon. The application ideas which prompted this investigation are discussed later. The following procedures will serve as an introduction to the problem:

1. Design and construct a high-vacuum system for purposes of testing various ceramic samples, and develop a source of free electrons to approximate a plane emitting surface.

2. Perform tests upon a variety of ceramic discs using in effect both diode and positive-grid triode testing circuits, and record the testing procedures used.

3. Record all pertinent data.

4. Make an analytical study of the experimental results and develop relationships among the parameters showing the effects of space-charge limiting, temperature or emission saturation, electron trapping, and area reduction, all of which affect the electron permeability of a porous ceramic.

5. Discuss possible application of this research to the design of highly reliable electron tubes.

6. Make suggestions which might guide future research in this area.

C. Review of Literature

Although an extensive search has been carried out over the last two years, no publications encompassing the subject of this thesis have been found. Material relating indirectly to the subject and to some of the experimental procedures involved herein are listed in Section VI under Selected References. Following is a brief review of such references.

Guidance concerning experimental apparatus and methods involving high-vacuum techniques is given in texts by Dushman (9) and Strong (32). The preparation and activation of oxide-coated cathodes is discussed by Spangenberg (31, p. 42-46) and by Kohl (18, chpt. 19). An article by Lafferty (19) describes the preparation of a lanthanum boride cathode that can be reactivated at 1500° C after having been opened to air.

Such reactivation is not possible with the usual oxide cathodes. Another cathode capable of reactivation, called the L-type or impregnated cathode, is described by Hill (14). This cathode has a plane-circular emitting area and operates at about 1150° C.

One of the most difficult parts of the experimental problem is that of obtaining a plane source of free electrons without excess heating. A possible solution is offered by using the positive grid of a triode device as the effective source of electrons. Electron-current division between the grid and plate is described in standard texts (3, 7, 31) and in published articles (6, 16, 30).

Since ceramic engineering is not widely studied by electrical engineers, some indoctrination in the field of insulators and refractory ceramics is necessary. The physical properties of the samples used will be given later. Textbooks by Newcomb (25) and Kohl (18, chpt. 15) offer excellent descriptions of the raw materials used, manufacturing processes and the physical properties of the resulting ceramics. An article by Lindsay and Berberich (20) discusses the conductivity of ceramics such as alumina porcelain. This particular insulator conducts by dielectric absorption below the critical temperature of 250° C and by electrolytic conduction above this temperature. The subject of dielectric breakdown has received considerable attention. Theories describing this temperature sensitive action are found in texts (11, 35). When insulators are stoichemetric (combined in the proper proportions) they have very high resistivities. Most insulators are somewhat like semiconductors since the imperfections lower the resistivity. Theories involving internal

energies are developed which indicate that for certain temperatures as the electric field increases an avalanche of electrons causes "breakdown." These theories are unsettled at the present time. Mott and Gurney (22), in their text, offer an excellent coverage of electron behavior in solids.

Research in the field of solid-state physics has been very active in recent years. Articles by Conwell (5) and Coblenz and Owens (4) represent such work. Since the problem at hand is to deal with electron action in the voids of ceramics, the internal conductive actions are not of primary importance. Electron trapping by closed pores or by energy traps may have some significance in certain materials. A. Rose (28), through private communication with the author, expects to publish some information concerning space-charge-currents through thin layers of cadmium sulfide in connection with photo-emission processes.

A very timely article by Navias (24) describes the advances in ceramics related to electron tube development. The ceramics are used as spacers and for structural purposes since the porous refractories outgas readily and are superior to mica and glass in many respects. Properties of various raw-material mixtures are discussed. Palmer (26) describes a commercially possible ceramic tube. The ceramic alumina spacers with dimensions controlled to 0.0005 inch replace the conventional mica spacers. The tube envelope is ceramic with a vitreous outside, permitting higher outgassing temperatures than the conventional glass. Operation at 400° C is permitted, while glass would melt under

similar conditions. Automatic assembly of this ceramic tube is explained.

Hydraulic engineers have studied the passage of gas and liquids through porous sand beds as reported in a text by Muskat (23) and in an article by Barrer (2). Darcy's law is an empirical equation governing the flow in porous media and is analogous to Ohm's law. The complete analogy is not possible since the limiting action of the electron-space-cloud has no counterpart.

Perhaps the publications most useful to the study of electron movement through porous materials are those dealing with the internal processes of an emitting oxide layer. These investigations were prompted by the inability of the Child-Langmuir equation and the Schottky effect to fully explain the current-voltage curves of a diode with an oxide-coated cathode. Loosjes and Vink (21) introduced the possibility of the porous coating containing space charges with emission from the sides of the pores and diffusion of the electrons to the oxide surface. Reasoning that the oxide coating must be conductive to restore the emitted electrons, they determined that 50 per cent porosity is about optimum. The activation process must be controlled very carefully if sintering and decreased porosity are to be avoided. The conductivity of the coating can be treated in two parts as shown by the two distinct slopes in the plot of the natural logarithm of conductance vs the reciprocal of temperature. Conduction of electron gas between grains of the porous coating plus the electronic conduction in the crystals of the coating are

taken as parallel processes. At low temperatures the crystal conduction predominates while the large current densities at the higher temperatures are mostly the electron gas. The cross-over temperature is about 800° K. No quantitative theory is available, although qualitative reasoning is presented. These principles are further advanced by Wright and Woods (36) using an accelerating field, and by Shindo (29) using both accelerating and decelerating fields. Hensley (12) reports on the electrical properties of porous oxides from a semiconductor point-of-view.

II. INVESTIGATION

A. Materials and Apparatus

The use of ceramics in the electron tube industry is expanding rapidly. Ceramic research has decreased the electrical losses so that ceramics can be used at frequencies up to 10,000 megacycles. Operating temperatures around 400° C are now possible using ceramic spacers and a vacuum-tight ceramic envelope. Another application uses a magnesia insulating sleeve with the heater embedded. This compact unit is then inserted inside of the tight-fitting oxide emitter. Ceramic cements are used and also the ceramic-to-metal seal is now possible. At comparable temperatures ceramics are superior to glass, because their crystalline structure reduces the electrolytic conduction present in the amorphous glass.

"Ceramics" is a very general word, derived from the Greek "Keramos", meaning potters' earth or clay. In more general terms ceramics are inorganic materials which are brought to permanent shape and hardness by high-temperature firing. Such a definition includes abrasives, cements, enamels, glass, clay products, refractories, terra cotta and white ware. Mica, a natural mineral, is not considered a ceramic.

The different combinations of the many raw materials result in a limitless number of ceramic compositions with a wide range of

characteristics. The most common ceramic ingredients are: alumina (Al_2O_3), silica (SiO_2), magnesia (MgO), thoria (ThO_2), beryllice (BeO), zirconia (ZrO_2), and carbon (C). The firing procedure and the firing temperature also determine the properties of the resulting ceramic.

As in any industry, the materials produced by the ceramic companies are designed to meet the needs of their customers. Accordingly, the ideal material needed for this experiment was not available from standard stock. The major ceramic companies were contacted and it was found that their most porous material, which was porous only because of the imperfect particle packing, was too dense for space-charge currents to penetrate, even under the influence of high electric fields. Such materials are exemplified by:

(a) Al/SiMag 548 American Lava Corporation, Chattanooga, Tennessee.

(b) Al-100 Coors Porcelain Company, Golden, Colorado.

(c) RA-84 Norton Company, Worcester, Massachusetts.

(d) Ceramic with randomly oriented organic hairs, specially prepared by the Ceramics Department of The Missouri School of Mines and Metallurgy, Rolla, Missouri.

Efforts to secure a ceramic similar to the Christmas-tree plastic, Styrofoam, resulted in the obtaining of the following six materials which were used as the principal test samples.

1. White fire-brick, B and W K-26, manufactured by the Babcock and Wilcox Company of New York. This material is shown in Figure 1(a) with a magnification of 40. It is designed for use in high temperature application where low thermal conductivity is required. An organic material

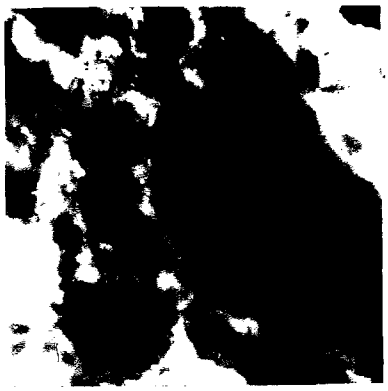

(a) White fire-brick
B and W, K-26

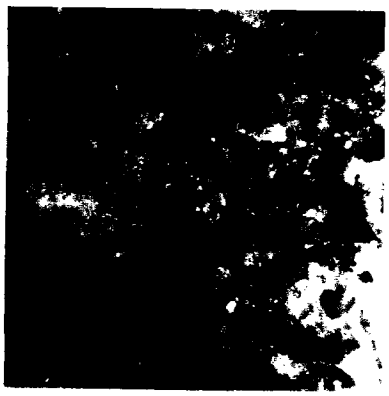

(b) Norton RA-98
filter disc

(c) Coarse-beaded
Al/SiMag 576

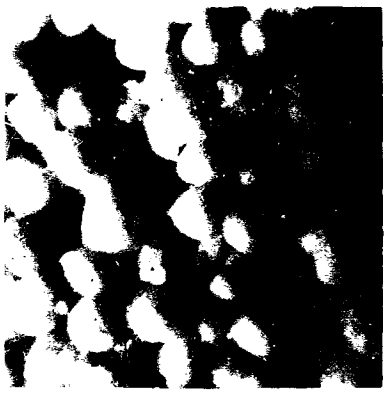

(d) Fine-beaded
Al/SiMag 576

Figure 1. Photomicrographs of porous materials used in experimental investigations with magnification of 40

such as ground cork or sawdust is included in the wet mold which when fired, results in an irregular porous structure. The fire-brick does not have good mechanical properties compared to other ceramics.

Babcock and Wilcox Bulletin R-2-H lists the following characteristics:

Service temperature	2600° F or 1428° C
Average weight	41.6 lb/ft^3 or 0.0241 lb/in^3
Fusion point	3000° F or 1650° C
Reheat shrinkage at 2550° F	0.4 per cent
Cold crushing strength	154 lb/in^2
*Porosity factor	0.515.

2. Ceramic gasoline-filter used in the gasoline lines of automobiles, manufacturer unknown. For purposes of this experiment, the filter bowl was ground into one inch diameter discs of various thicknesses. No manufacturers' data were obtained and the following characteristics were calculated:

Average weight	0.0485 lb/in^3
Porosity factor	0.83.

This material has a tendency to vitrify at lower temperatures than the other samples, which indicates a higher silica content.

---

*The porosity factors of the various materials were determined locally by reducing the material to its grain size and taking the ratio of the grain volume to the structural volume before crushing.

3. Norton RA-98, manufactured by the Refractories Division of the Norton Company, Worcester, Massachusetts. This coarse grade alundum filter disc is shown in Figure 1(b). These discs were intended to be used for filtering small amounts of solid matter from liquids by retaining particles of 20 microns. The following characteristics are taken from a Norton bulletin:

Melting point	2050° C
Expansion coefficient	68 x 10^{-7}/° C
Resistivity for the range 528° C to 1020° C	130 x 10^{6} to 1.8 x 10^{6} ohm-cm.
Porosity factor	0.98.

The porosity factor of 0.98 indicates the porosity is obtained simply by the imperfect packing of the crystalline grains.

4. Coarse-beaded A/SiMag 576, obtained through the helpful cooperation of the American Lava Company, Chattanooga, Tennessee. This very interesting material is shown in Figure 1(c). The discs of this novel material are made porous by first making individual vitrified alumina beads and then reheating them until adjacent balls just sinter together in a predetermined form. The resulting structure has excellent mechanical strength and high porosity, with very few closed pores. Before sintering, the beads are sifted and, in this case, are classified as -30 to +60 mesh size. This means that beads larger than 0.59 mm. in diameter are rejected. The basic material in the beads is a A/SiMag 576 and has the following characteristics as found in the A/SiMag chart No. 544:

Mesh size	-30 to +60
Water absorption	0 to 0.02 per cent
Density	0.123 lb/in^3
Softening temperature	2624° F or 1440° C
Coefficient of expansion	$7.5 \times 10^{-6}/^\circ C$
Compressive strength	150,000 lb/in^2
Dielectric strength	250 volts/mil
Resistivity at 100° C	2×10^{13} ohm-cm.
Resistivity at 900° C	4×10^5 ohm-cm.
Dielectric constant	8.2
*Hardness	9
Porosity factor	0.564.

By assuming ideal spacing and uniform spheres of radius R, it can be shown that for a cubic array the volume of the unit cell is 8 R^3 and the pore volume is $3.81R^3$ with a resulting porosity factor of 0.4764. For rhombohedral placing of the spheres the porosity factor is $1.47R^3/5.66R^3$ or 0.2595. In actual cases the sphere size and the spacings are not uniform, as verified by Figure 1(c), and theoretical calculations are not accurate. These calculations show that in the

---

*The hardness is measured on Mohs's scale where diamond is 10.

ideal case the porosity is independent of the particle size. It is also evident that in a practical case the sphere size should be quite uniform if high porosity is desired.

5. Fine-beaded A/SiMag 576, basically similar to the preceding coarse-beaded material. This material is shown in Figure 1(d). Its characteristics are:

Mesh size	-60(0.25mm) to +100(0.149mm)
Porosity factor	0.594.

6. Crucible disc from Coors Porcelain Company. This represents an artificially porous type of disc ordinarily used in chemistry laboratories.

Diameter of cylindrical holes	0.0282 inch
Average hole area	10 per cent.

The apparatus used in the experimental investigations is shown in Figure 2 and is identified by a numbering system. The vacuum system worked unexpectedly well. The fore-pump or rough pump was a Cenco-Hyvac mechanical pump capable of pumping to pressures of about 10 microns (10×10^{-6} meters of mercury). The fine pump was an air-cooled oil diffusion pump manufactured by Consolidated Vacuum Corporation, Type VMF-10. While the ultimate pressure of the system was 0.001 micron, the typical vacuum tube pressure of about 0.05 micron was used in the many tests. The time of an experimental cycle, caused by changing of samples and re-evacuation, was approximately two hours. Two vacuum gages were used to cover the range of pressures encountered. A National Research

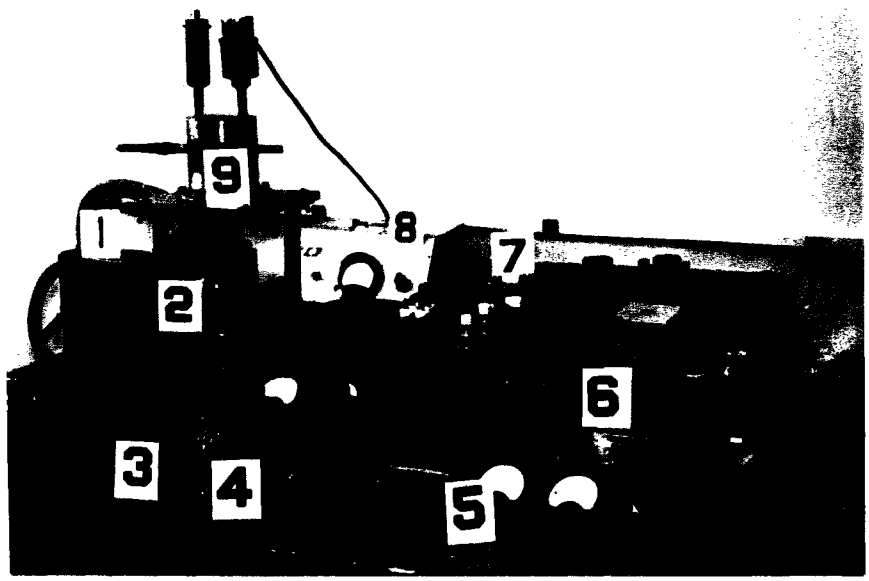

Figure 2. Experimental apparatus

(1) Mechanical vacuum pump
(2) Oil diffusion vacuum pump
(3) Cooling blower
(4) Control variacs
(5) Measuring instruments
(6) D-C voltage supplies
(7) Thermocouple bridge
(8) Philips gauge
(9) Vacuum chamber

Corporation Model 501 thermocouple gauge, with a pressure range of one to 1000 microns, was used. The high vacua were measured by a Philips Ionization Gage, Type PHG-1. Two scales covered the pressure range from 25 to 0.02 microns.

The vacuum chamber which contained the test samples is shown in Figure 3. This working drawing was used by the College Instrument Shop to construct the brass "bell-jar". The top was fastened to the base plate by eight screws and the vacuum seal was accomplished by a sunken teflon ring. The electrical connections were furnished by six Stupakoff Kovar seals rated at 5000 volts and 10 amperes.

The most challenging and difficult part of the experimental apparatus was the spacing and holding of the equivalent tube elements, particularly the cathode. A plane system of electrode spacing was used throughout.

The ideal cathode for this investigation would have a low-power input, a heat-shielded plane emitting surface about 1/2 inch in diameter, and adequate electrical isolation from all other electrodes. Of prime importance would be the possibility of its continued use after having been used and later exposed to air. As in most engineering problems these conditions could not be fully met simultaneously.

The first system tried consisted of a lava dish two inches in diameter and 3/8 inch thick. Lead holes and a cathode recess were formed while the material was in a soapy or unfired state. The dish was then fired at temperatures around 1400° C and became hard but was still capable of being outgassed. Satisfactory methods were devised to

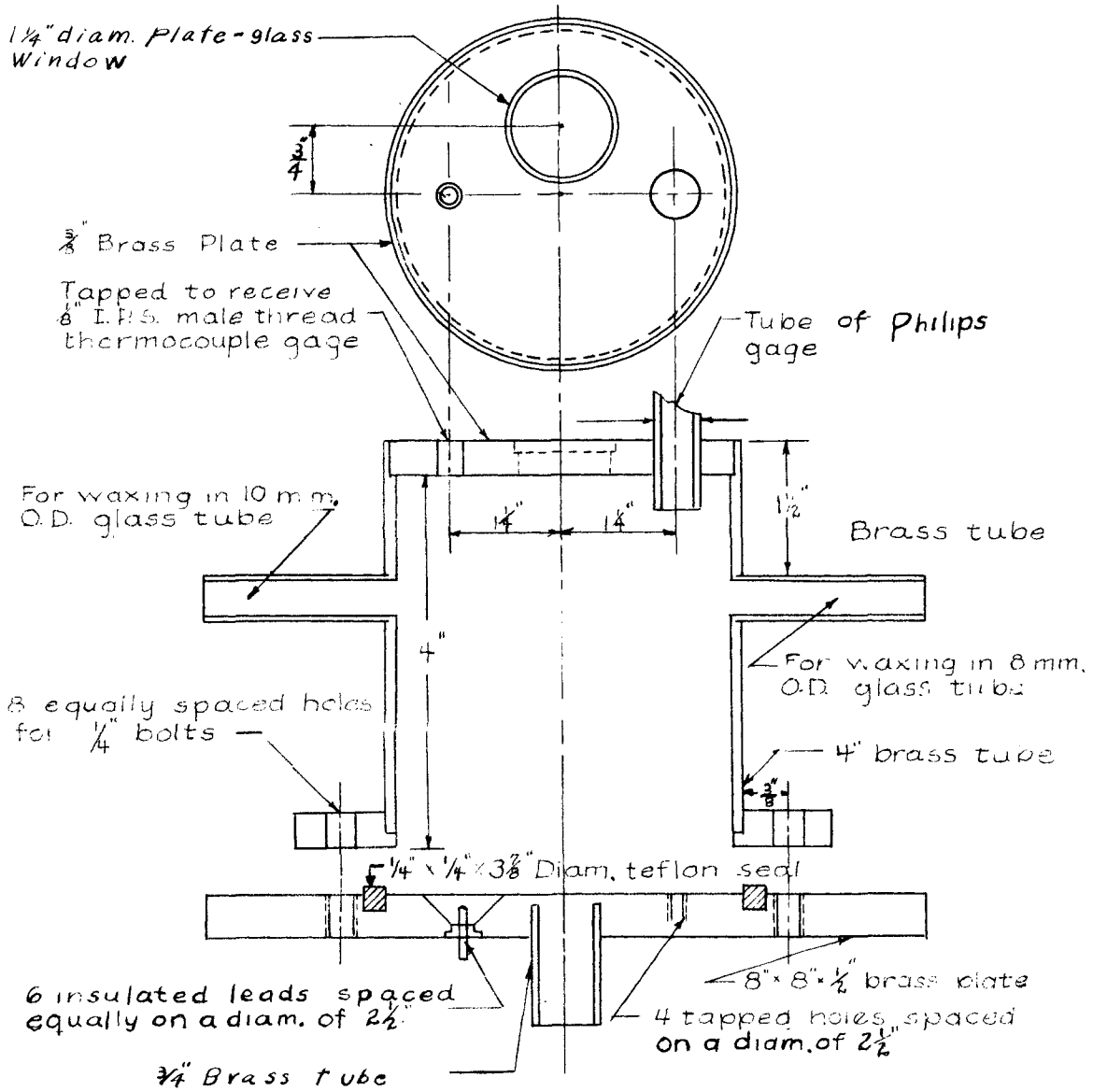

Figure 3. Working drawing of vacuum chamber

hold the elements, including the various cathodes. The dish was held about one inch from the brass base plate by three brass pins. The difficulty came through the lack of sufficient heat sinks. This means that the temperature of the entire system became excessive after a time determined by the filament power. The excessive temperatures caused the soldered connections to vaporize. When this was eliminated, vaporization of other system parts also gave trouble. This method using the ceramic dish was finally abandoned.

The elements were next inverted so that the plate was located near the cool base plate and separated from it by a thin piece of porcelain. The test sample was held in its place over the plate by an aluminum ring which was cooled also by contact with the grounded base plate. The cathode with its heat shields was then suspended over the sample without actually touching it. The result was that the cathode structure got hot but, except for heat radiation, was isolated from the other parts. This cathode isolation also offered a guarantee that the plate current was truly electron current since no path for conduction current then existed.

A great amount of time was spent perfecting four or five different cathodes. Without going into extensive details, the following summary may prove helpful to others in need of experimental cathodes. The oxide-coated cathodes are well known for high emission efficiency and for their low operating temperature. The most serious disadvantage is the inability of the oxides to remain active after being exposed to air. The activation process is considered an art rather than a science, because

the heating cycle and the aging with plate voltage applied, greatly affect the emission. Variations in the temperature-limited emission occur due to aging and are troublesome except where space-charge-limited currents are used.

Two shapes of directly heated oxide filaments were used in early tests. Filament material used in the familiar 5U4 vacuum tube was obtained from the General Electric Tube Works in Owensboro, Kentucky. The filament coating is a triple carbonate put on by an electro-deposition method. This method has proven superior to drag coating since it does not flake off as much when handled and shaped. The base metal is composed of 54.0 to 55.5 per cent nickel, 44.0 to 45.5 per cent cobalt with traces of iron and silicon. Between 10 and 40° C it has a temperature coefficient of resistance of 0.0032 and a ribbon weight of 187 milligrams/200 millimeters. The ribbon base is rectangular, measuring 0.006 inch by 0.044 inch. The first filaments were made from five inch lengths in the form of spirals and were activated and operated near a voltage of three volts and a current of 4.5 amperes. The second oxide-coated filament was formed by a series of bends which resulted in a flat emitting surface consisting of seven 3/4 inch strips side by side. These cathodes were difficult to shape. Since they could not be reused and because of the continually changing emission the oxide cathodes were abandoned.

Another attempt to obtain a plane emitting surface, which could be reactivated, was the use of lanthanum boride as described in an article

by Lafferty (19). A temperature of approximately 1500° C is required to sinter the boride into the graphite base while the operating temperature is about 1150° C. It was found that to maintain these temperatures over the surface area, a prohibitive amount of filament power was required. An optical pyrometer was used in making temperature measurements.

The fourth cathode used was the "L-Type" described by Hill (14). It is capable of reactivation at an operating temperature of 1150° C. Satisfactory emission was obtained from a 1/2 inch diameter cathode but the internal heater power of about 30 watts created heating effects that caused the data to be erratic.

The cathode finally used in obtaining the data presented in a later section was a short spiral tungsten wire. This choice represents a compromise between filament power and uniform plane emission. A two inch piece of 8.5 mil tungsten wire was wound into a spiral and fastened in the open end of a 1/2 inch cylindrical heat shield. The filament was heated to remove any initial stresses and was then reshaped while hot into a uniform spiral. Since the same cathode unit was used in successive tests, delicate handling was required to preserve the brittle and fragile tungsten wire. The fastening of the tungsten wire (to operate at about 2000° K) without the aid of refined spot welding techniques was a major obstacle. Pressure contacts between metals proved to be satisfactory.

Measurements were made with standard laboratory instruments with protection against occasional arcing. The high voltage was supplied by a 2500 volt transformer wired as a voltage tripler with a variac input.

B. Method of Procedure

Using the apparatus described in the preceding section, two general types of investigation were conducted.

The first, hereafter called the "diode test", consisted primarily of determination of the plate characteristics of a "diode" consisting of the spiral tungsten filament and a "plate", with the porous ceramic sample between the two electrodes. The wiring diagram used in the diode tests is shown in Figure 4, and the symbols there are used in the presentation of results. The 50-mesh screen, used as the accelerating plate, allowed for the installation of a reflector just back of it. As the electrons approached the mesh some would continue their flight and be collected or repelled by the reflector. Reflector current was recorded as a function of the reflector voltage for use in analyzing the velocity distribution of the electrons reaching the plate.

The second type of investigation, called the "triode test", used the circuit shown in Figure 5 to collect data to supplement those found in the diode tests. In this case the emitted electrons were given initial velocities determined by the grid voltage V_g. Some electrons continued into the test sample to be accelerated by V_p while the remainder terminated at the grid, as measured by I_g. The symbols shown in Figure 5 will be used in the remainder of the text to describe the triode data.

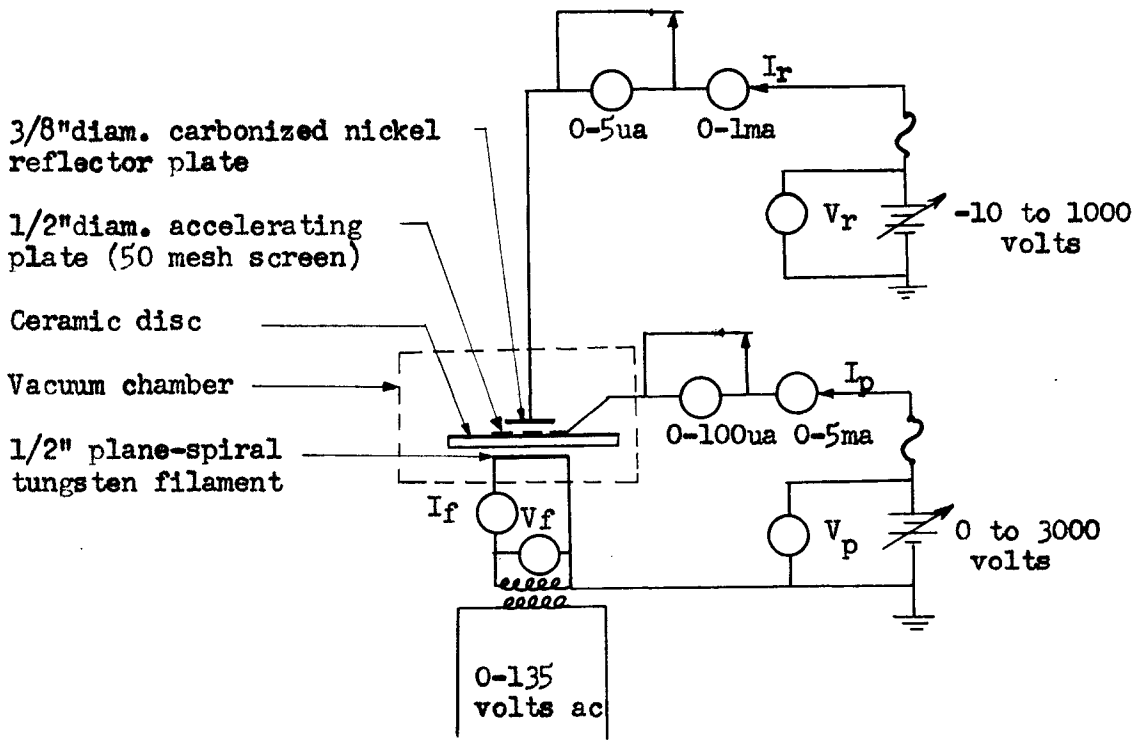

Figure 4. Wiring diagram used for diode tests

A typical experimental run consisted of first assembling the triode or diode device and then checking for filament continuity and for unwanted short circuits. The brass cap was then placed over the device and made vacuum-tight. The mechanical pump was started and after a 10 minute delay the oil diffusion pump and blower were activated. When the pressure was reduced to about 0.3 micron, the pressure for maximum

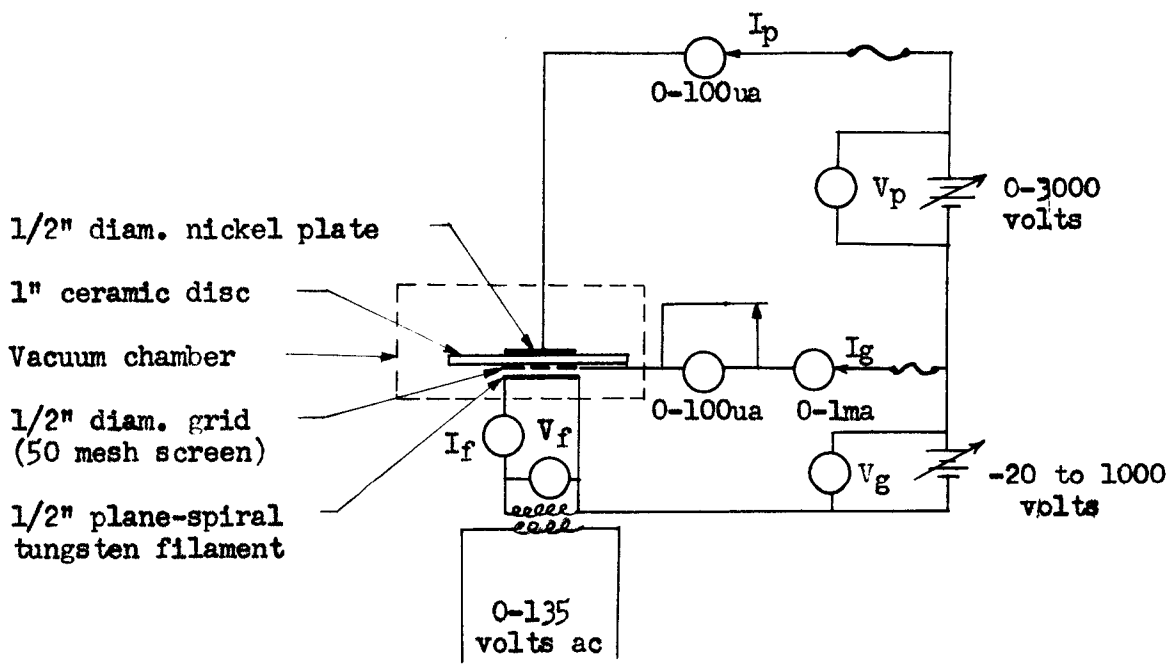

Figure 5. Wiring diagram used for triode tests

pumping speed, some filament power was applied to assist in quick outgassing of the system. Data runs were taken after the pressure decreased below 0.06 micron and after the filament action stabilized. As a precaution against interruptions, the variable voltage was increased to the maximum desired and readings were recorded as the voltage was decreased in steps. For each of the many samples tested, several runs involving different filament power were taken. After the filament of the test

device and the diffusion pump heater had cooled, the rough pump was turned off and the system was opened. In an effort to obtain better data near cut-off, a sensitive microammeter was shorted with a normally closed switch and placed in series with a higher-reading meter. During the run when the current had decreased sufficiently the switch was manually opened, providing more accurate readings.

III. RESULTS

A. Experimental Data

The data presented graphically in this section represent tests on a variety of porous materials, with measurements upon the different materials presented in a consecutive fashion so that the effect of different disc thickness can be readily observed. The plotted points represent experimental data and the curves approximate the trends. Things to observe while studying these data are: (1) The voltage at which the currents are zero, (2) the point where temperature limiting of the cathode starts, (3) the effect of filament voltage or total emission upon the shape of the curve, and (4) the imaginary positions of the curves with no ceramic disc present.

Figures 6 through 18 are results from diode tests involving the five major materials of Section II A which gave positive results. The Norton RA-98 material, Figure 1(b) does not transmit electrons with applied voltages up to 3000 volts. This last observation insures that no edge effects or leakage of electrons in the system was present during the tests which gave positive results. Figures 19 through 23 are results from triode tests with and without the coarse-beaded discs.

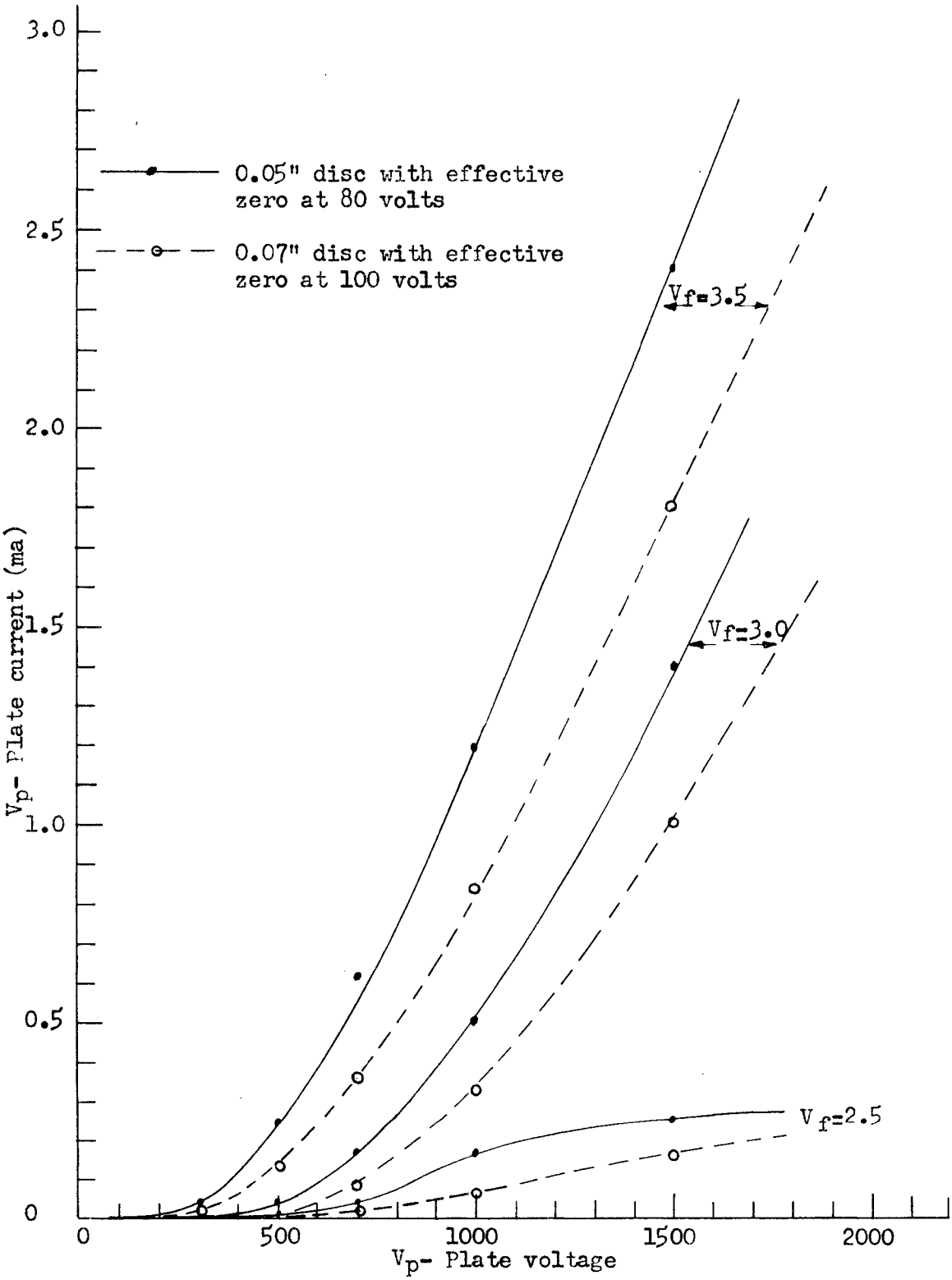

Figure 6. Plate characteristics of a diode device using white fire-brick discs

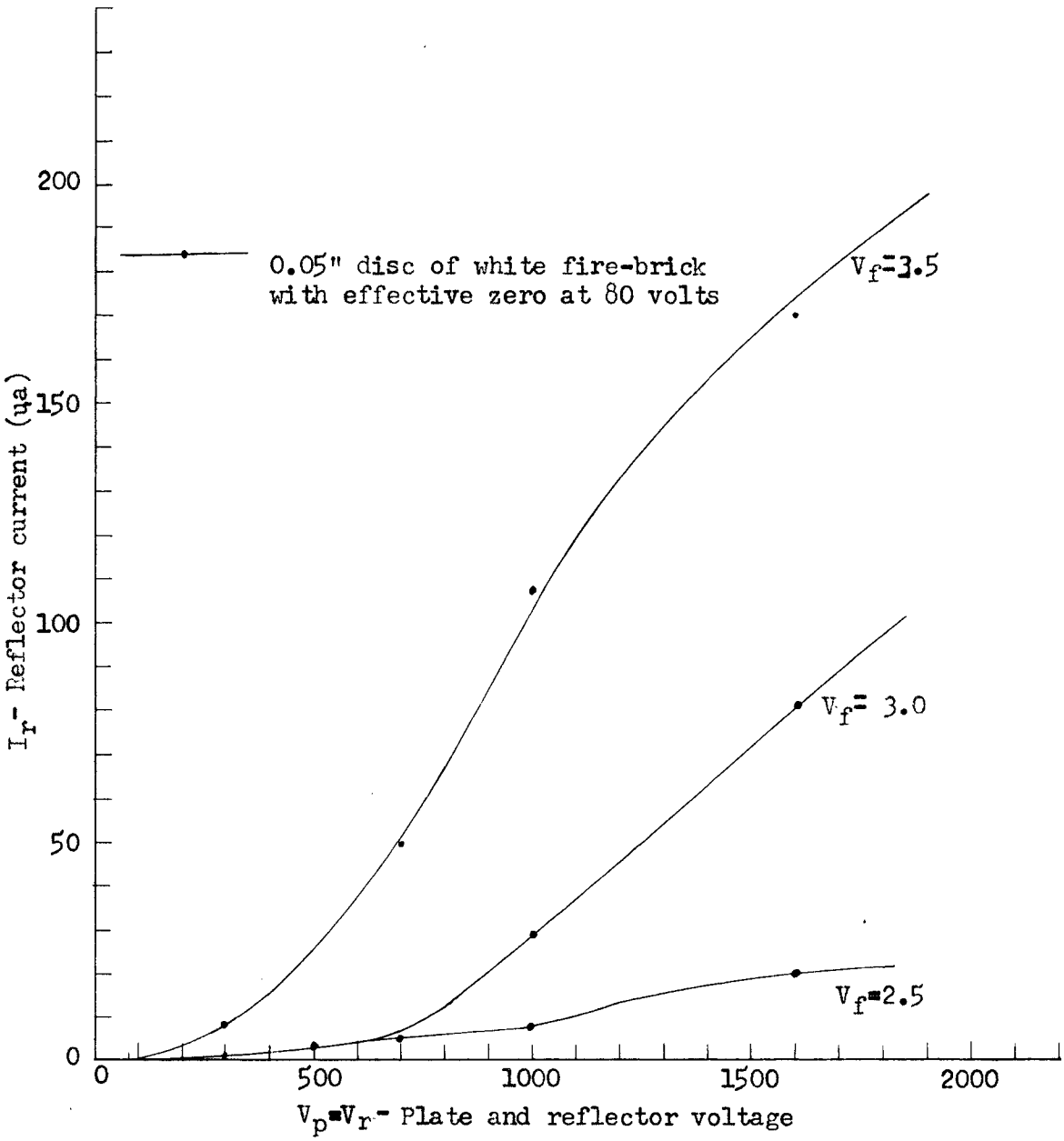

Figure 7. Reflector currents corresponding to curves of Figure 6.

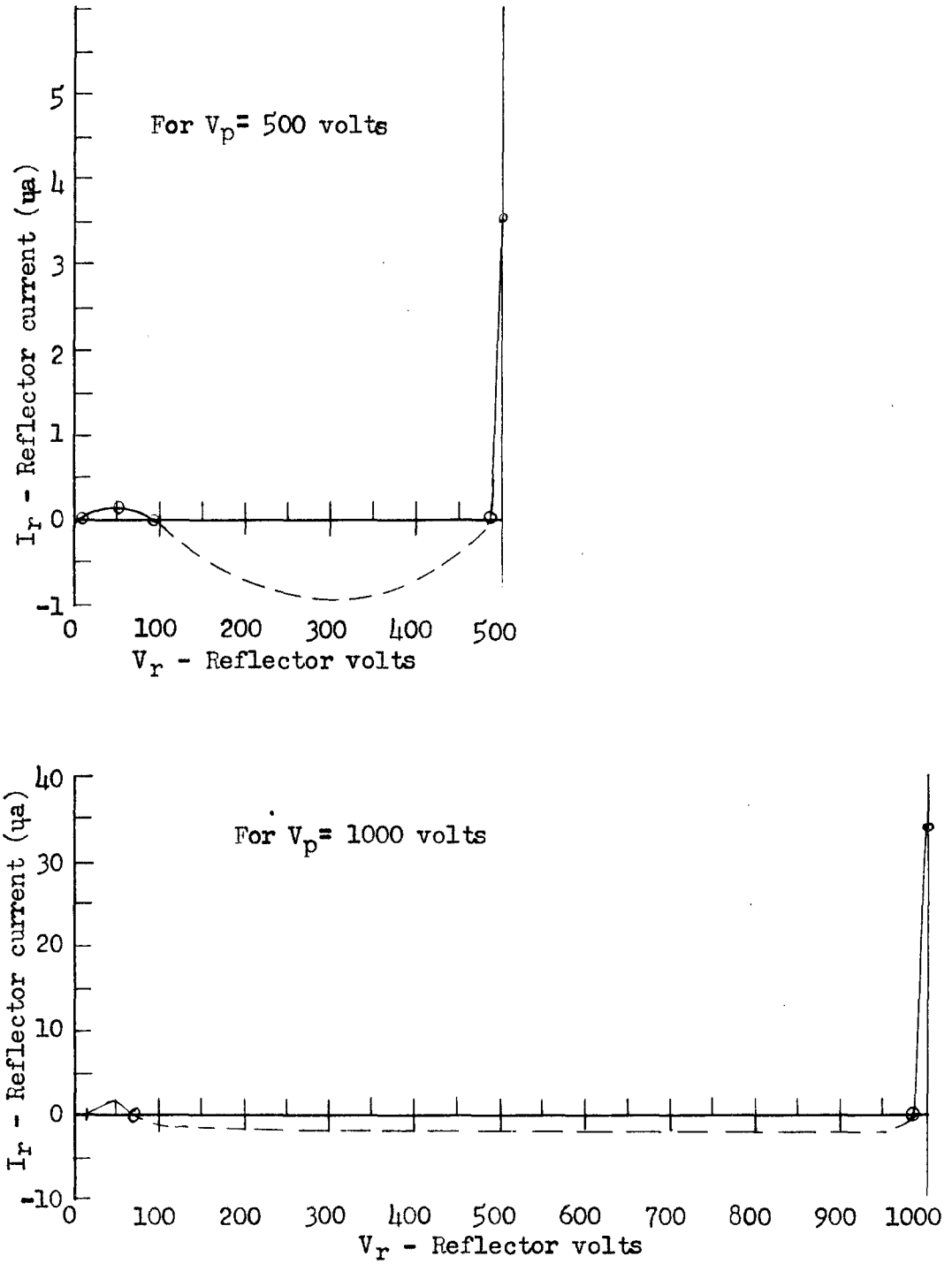

Figure 8. Reflector current vs reflector voltage for use in evaluating velocity distributions (0.07" fire-brick disc, V_f=3)

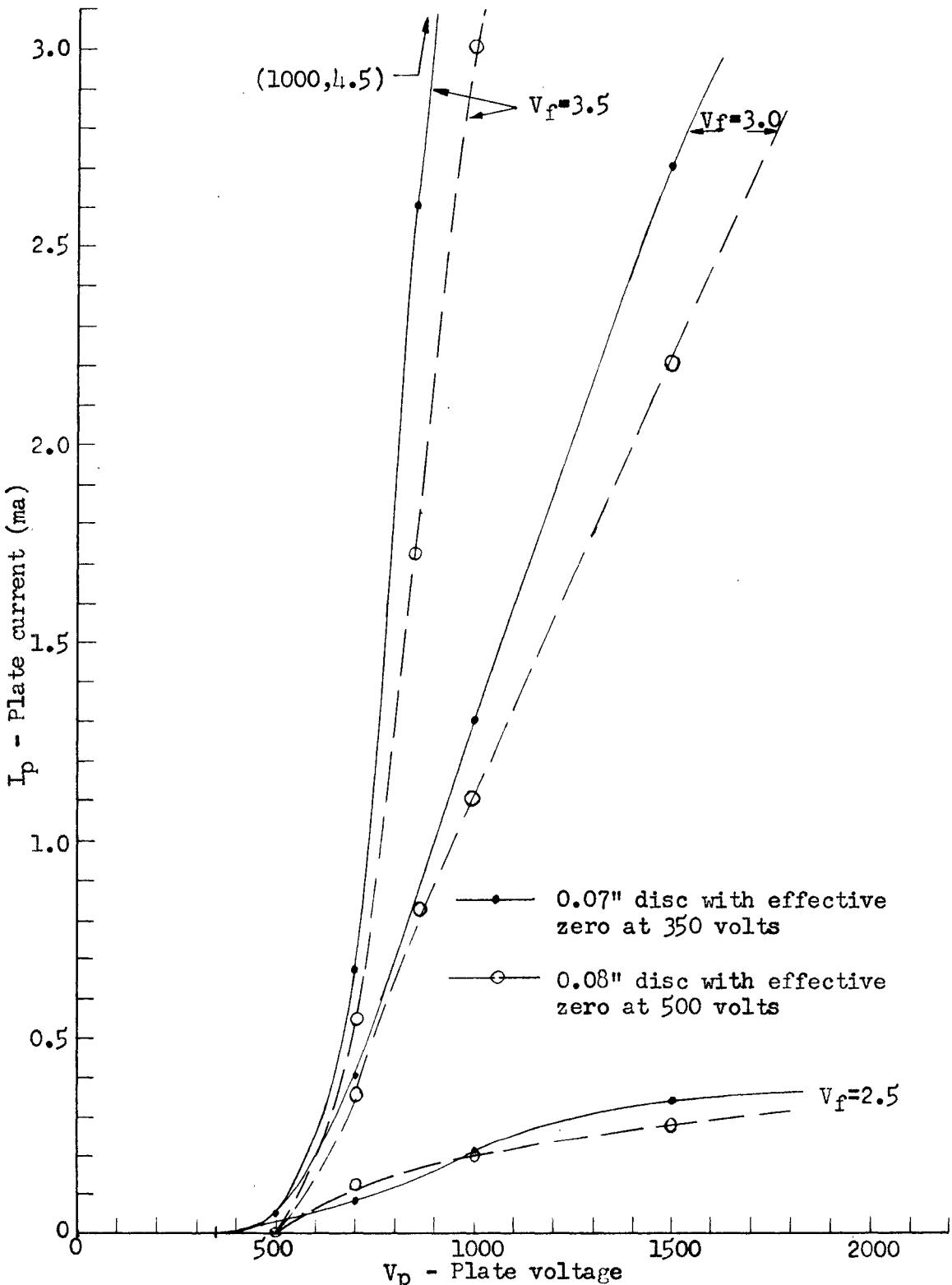

Figure 9. Plate characteristics of a diode device using ceramic gasoline-filter discs

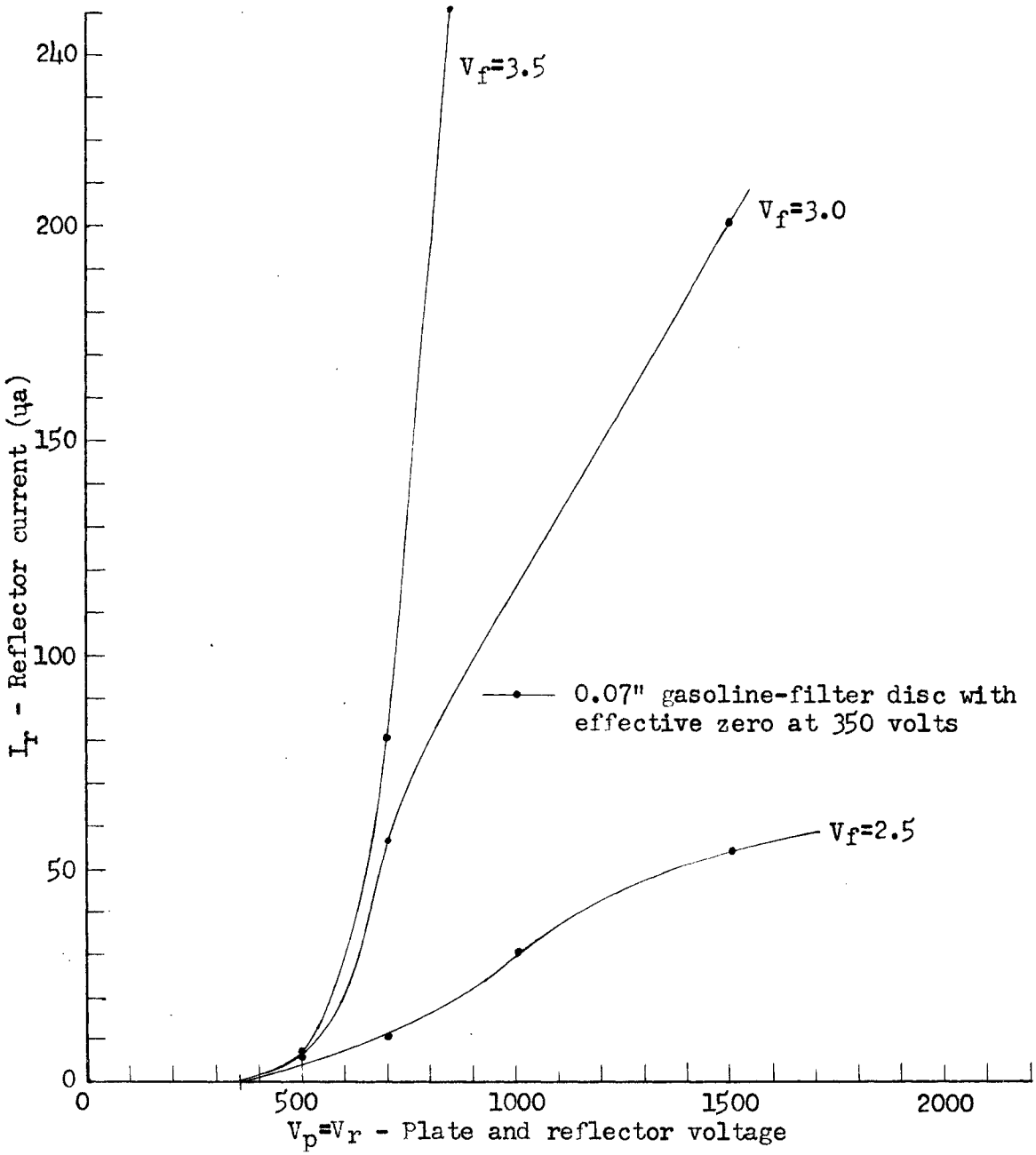

Figure 10. Reflector currents corresponding to curves of Figure 9

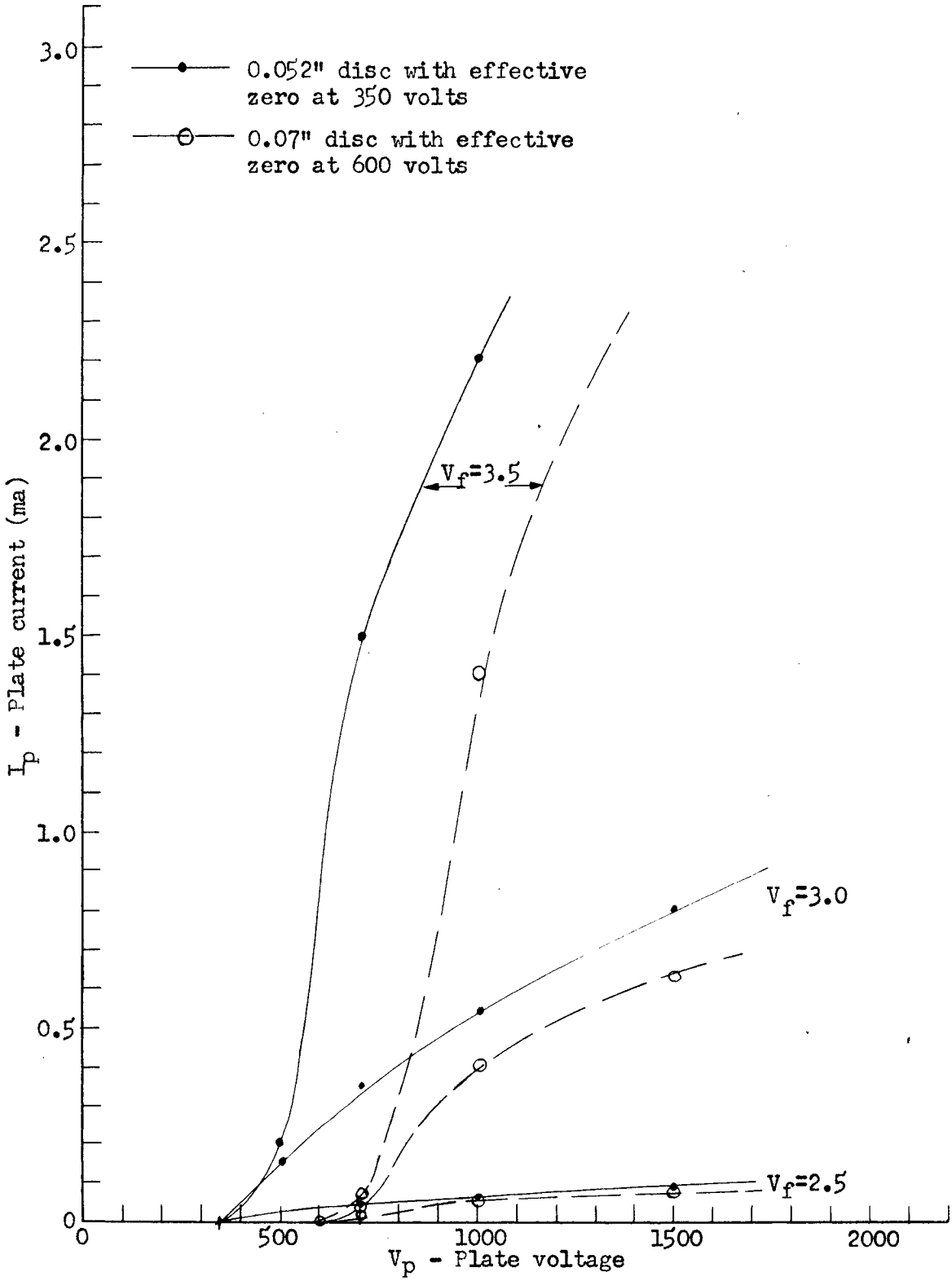

Figure 11. Plate characteristics of a diode device using coarse-beaded ceramic discs

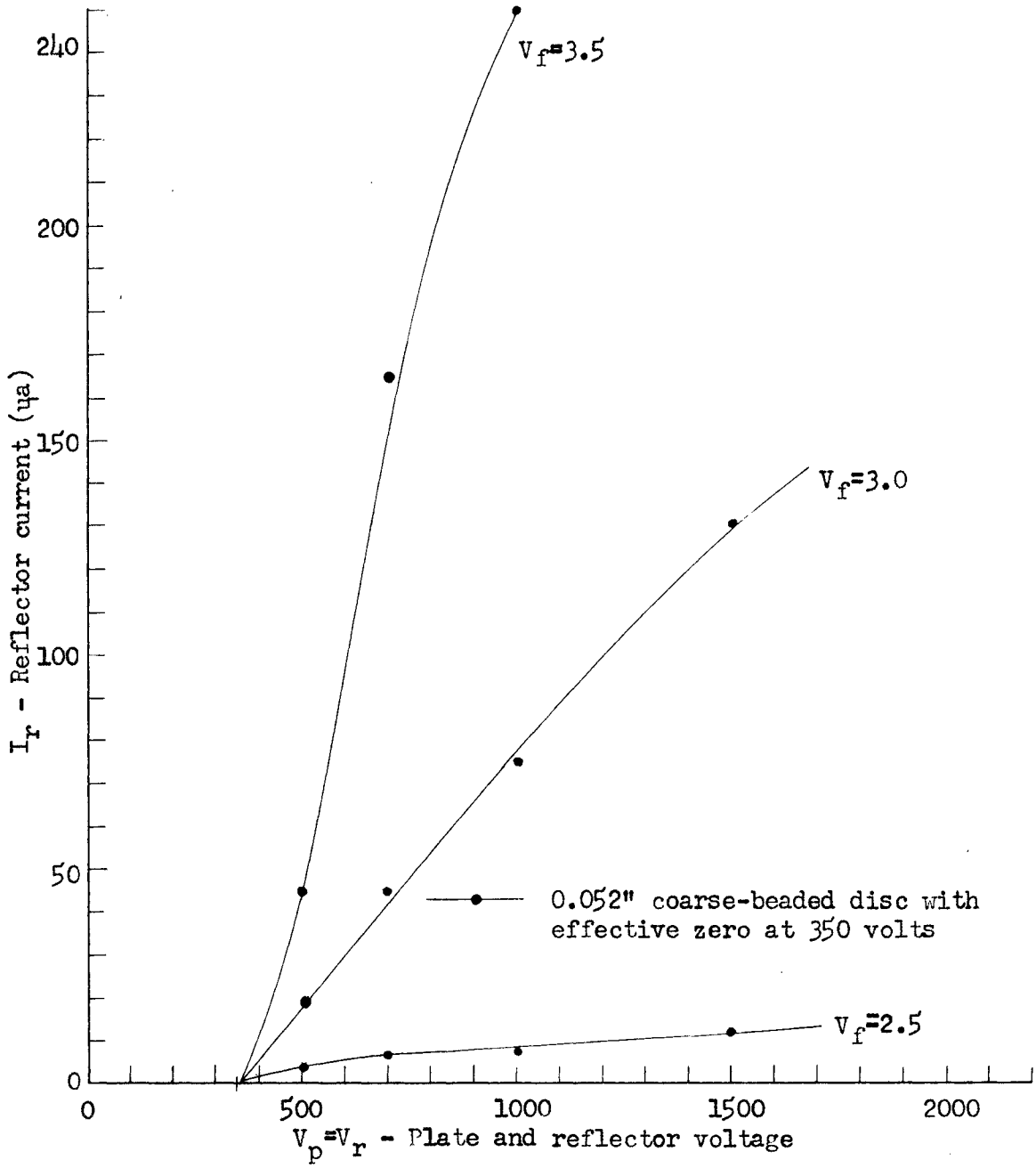

Figure 12. Reflector currents corresponding to curves of Figure 11

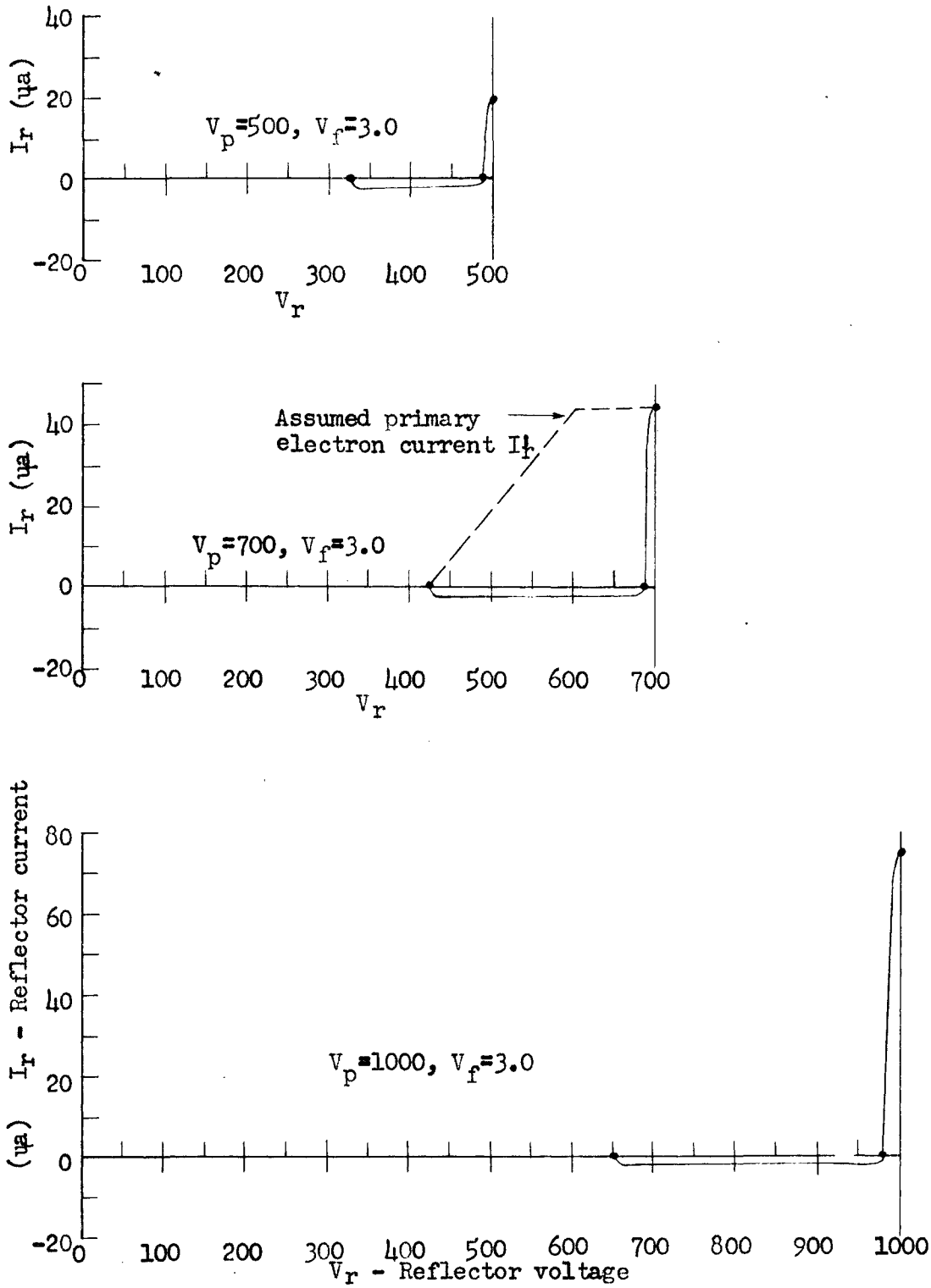

Figure 13. I_r vs V_r curves for use in evaluating velocity distributions (0.052" coarse-beaded)

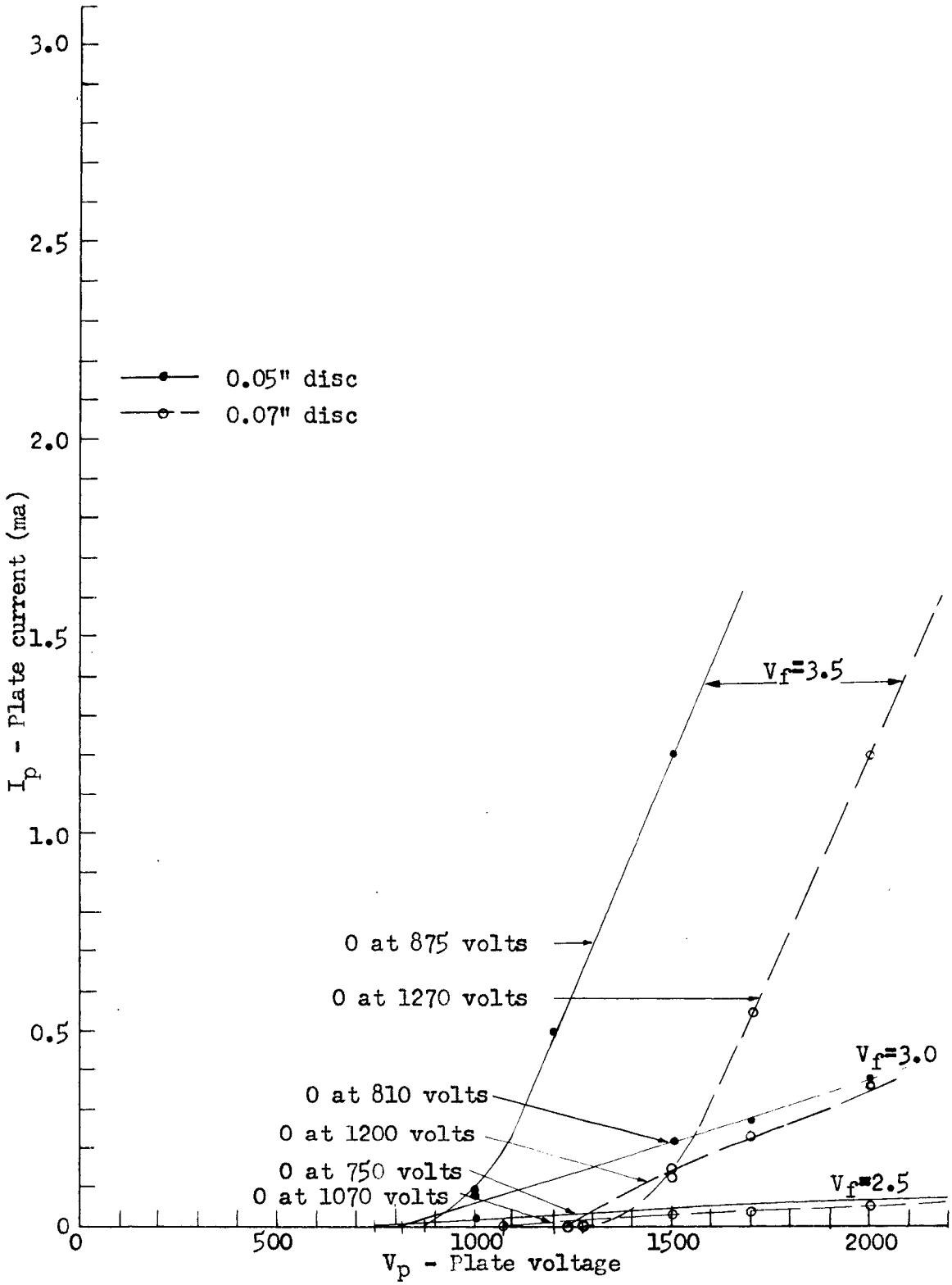

Figure 14. Plate characteristics of a diode device using fine-beaded ceramic discs

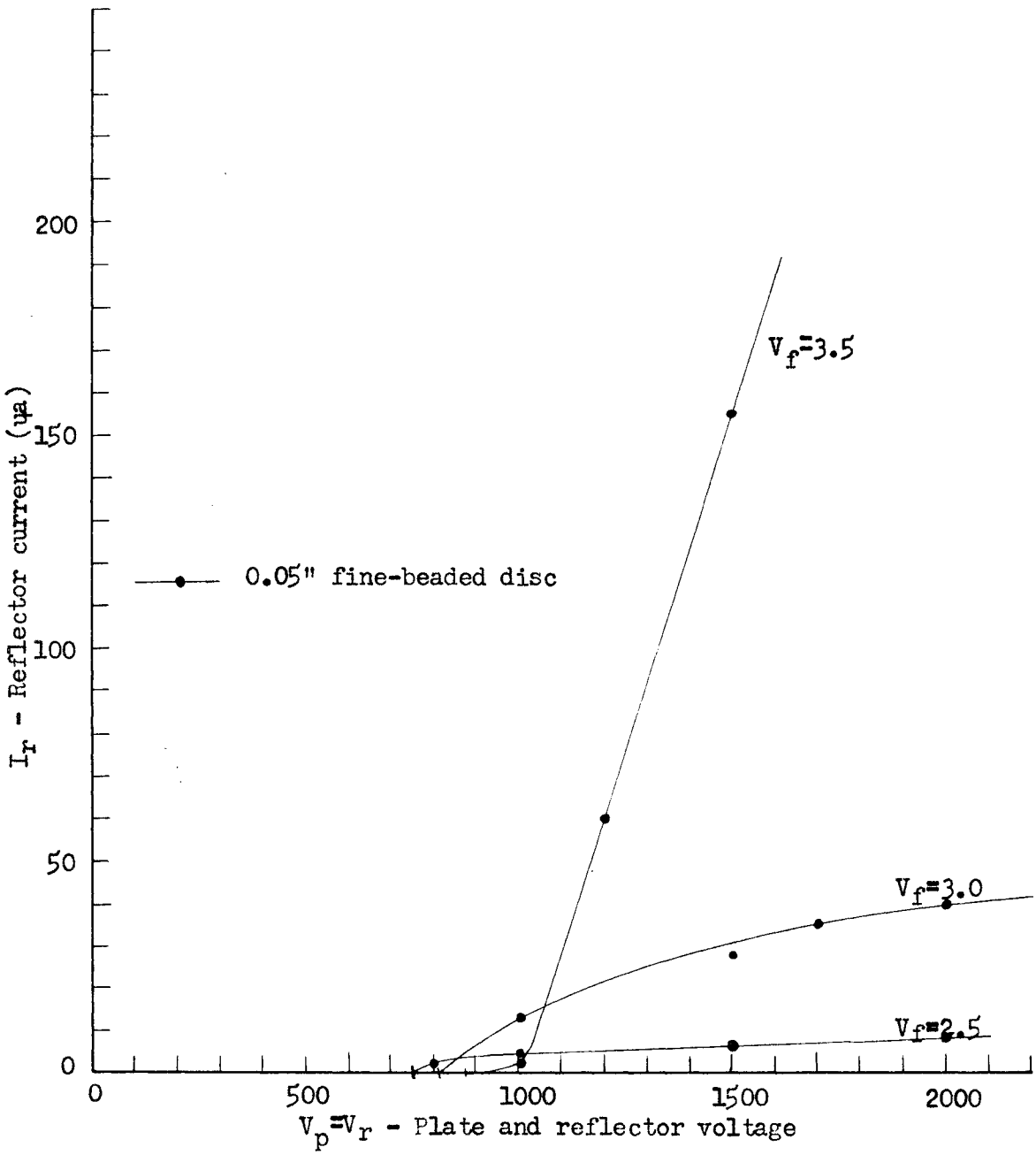

Figure 15. Reflector currents corresponding to curves of Figure 14

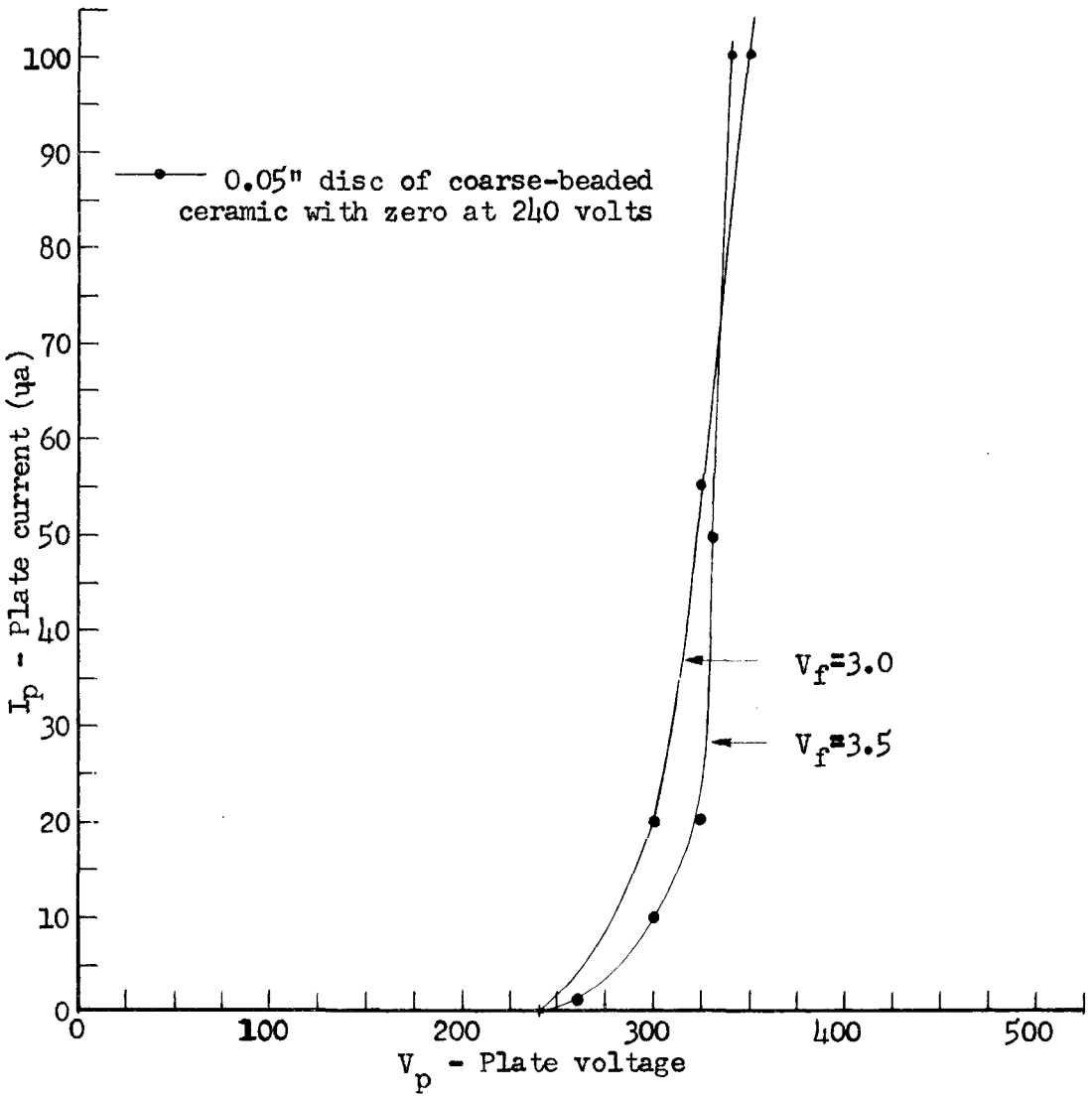

Figure 16. Enlarged examination of plate characteristics near cutoff

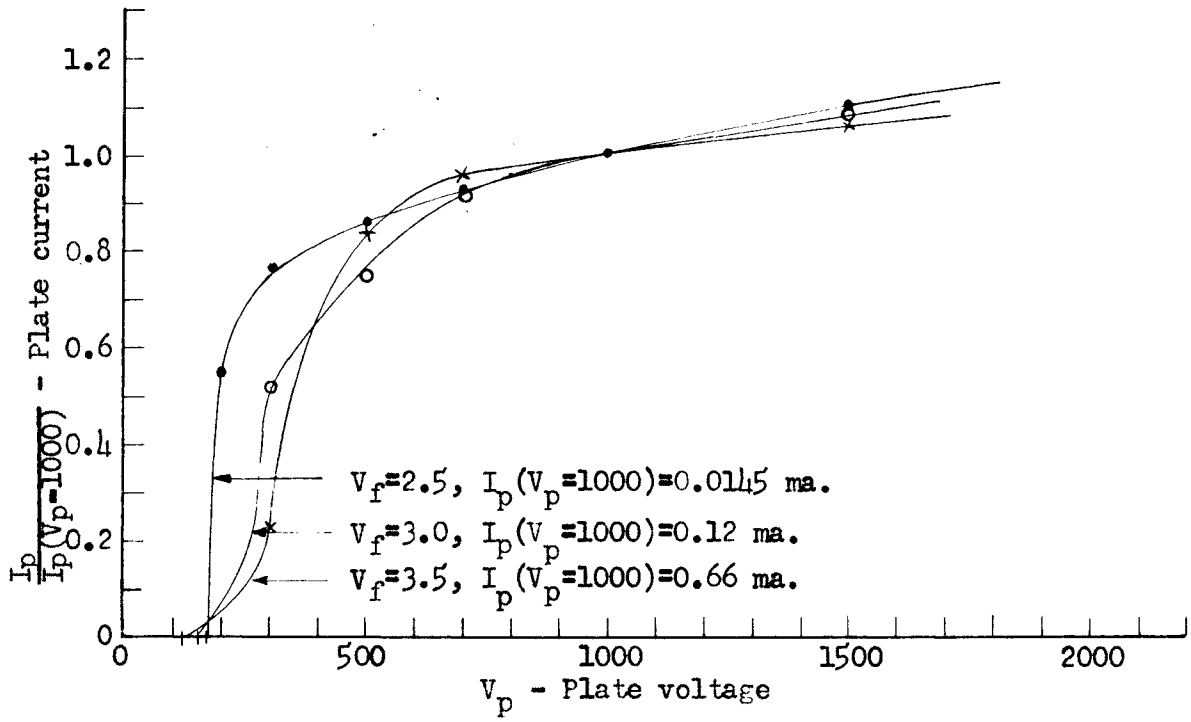

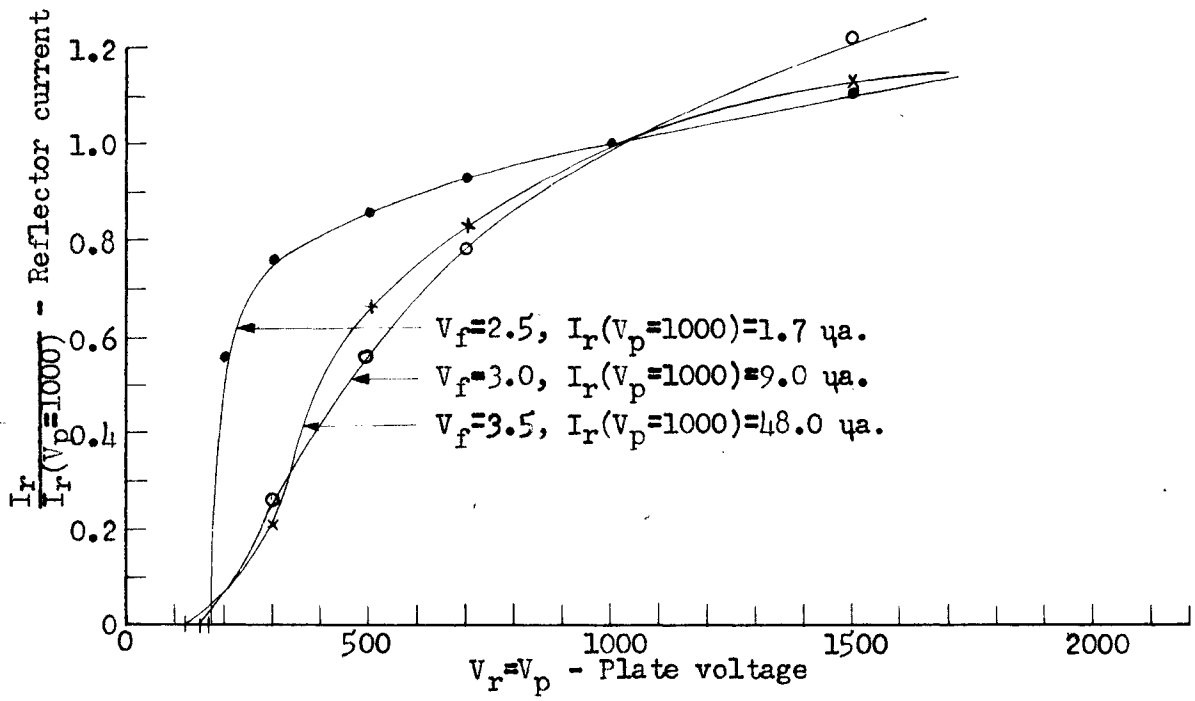

Figure 17. Normalized plate and reflector currents of a crucible sieve with holes (0.0282" diameter) averaging 10 per cent of the area with disc thickness of 0.062"

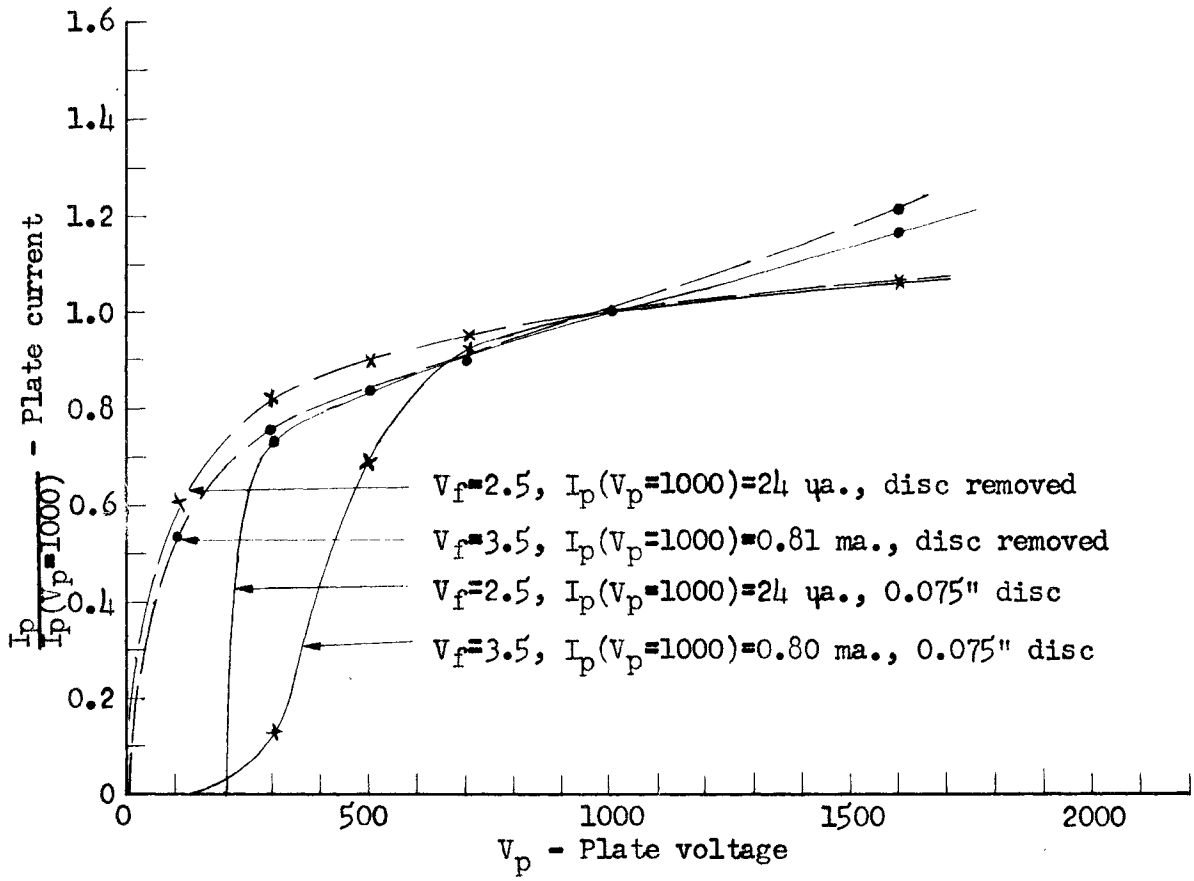

Figure 18. Normalized plate currents with and without crucible sieve having holes (0.0282" diameter) averaging 10 per cent of the area with disc thickness of 0.075"

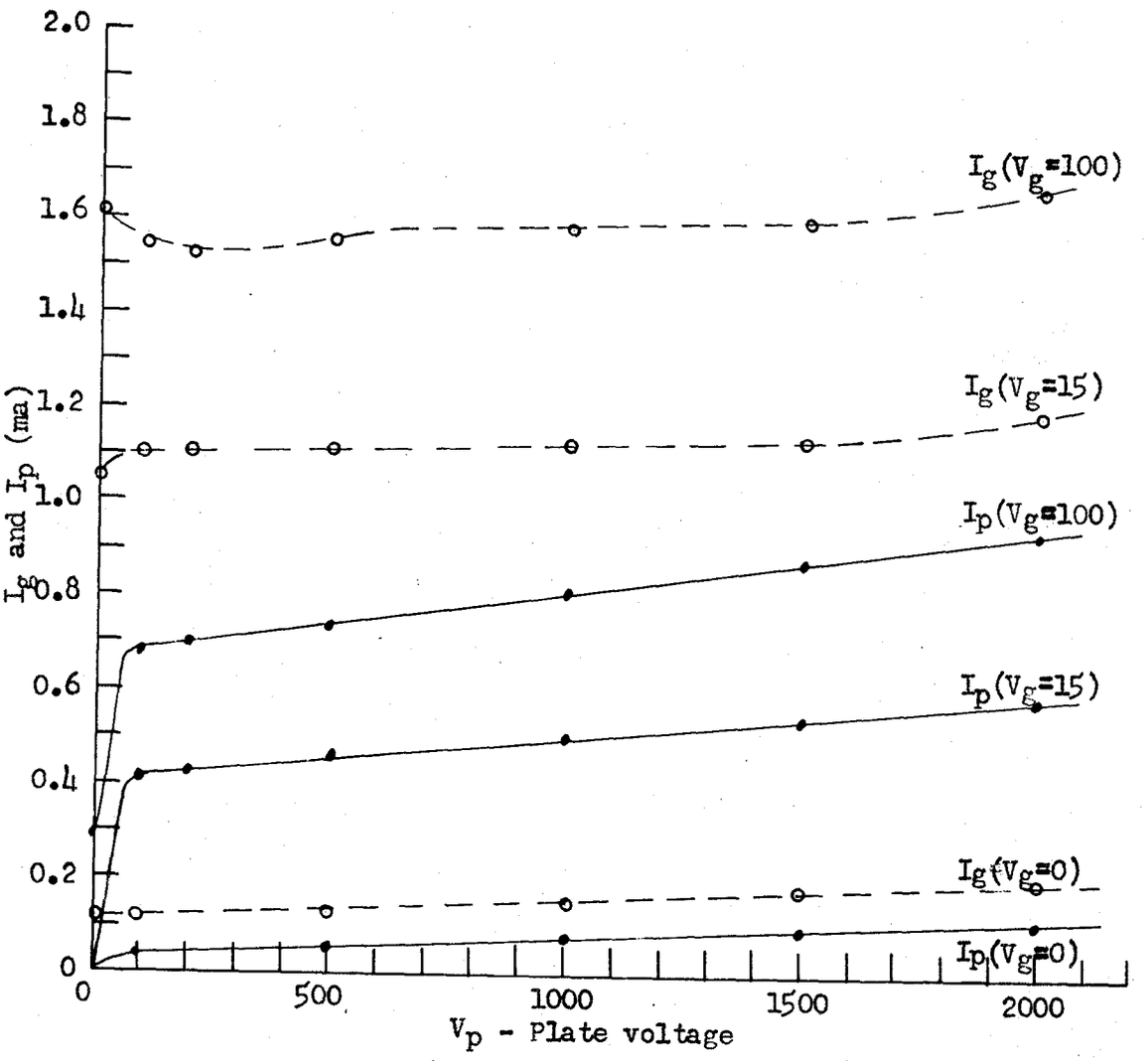

Figure 19. Triode characteristics for positive grid voltage (V_g) when no ceramic disc is present with $V_f=4$ and $I_f=4.2$

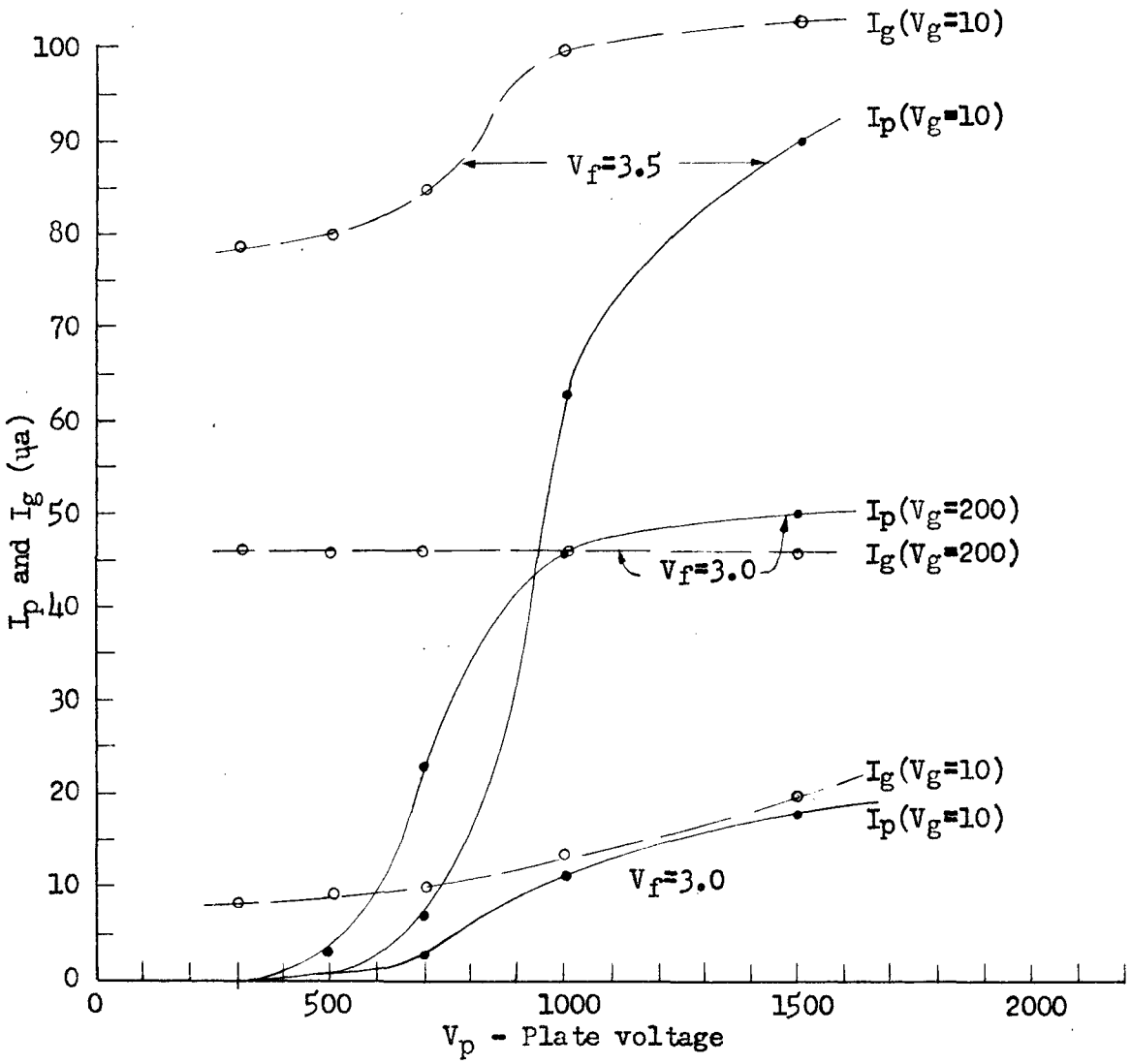

Figure 20. Plate characteristics of a triode device with a 0.07" disc of coarse-beaded ceramic between the grid and plate

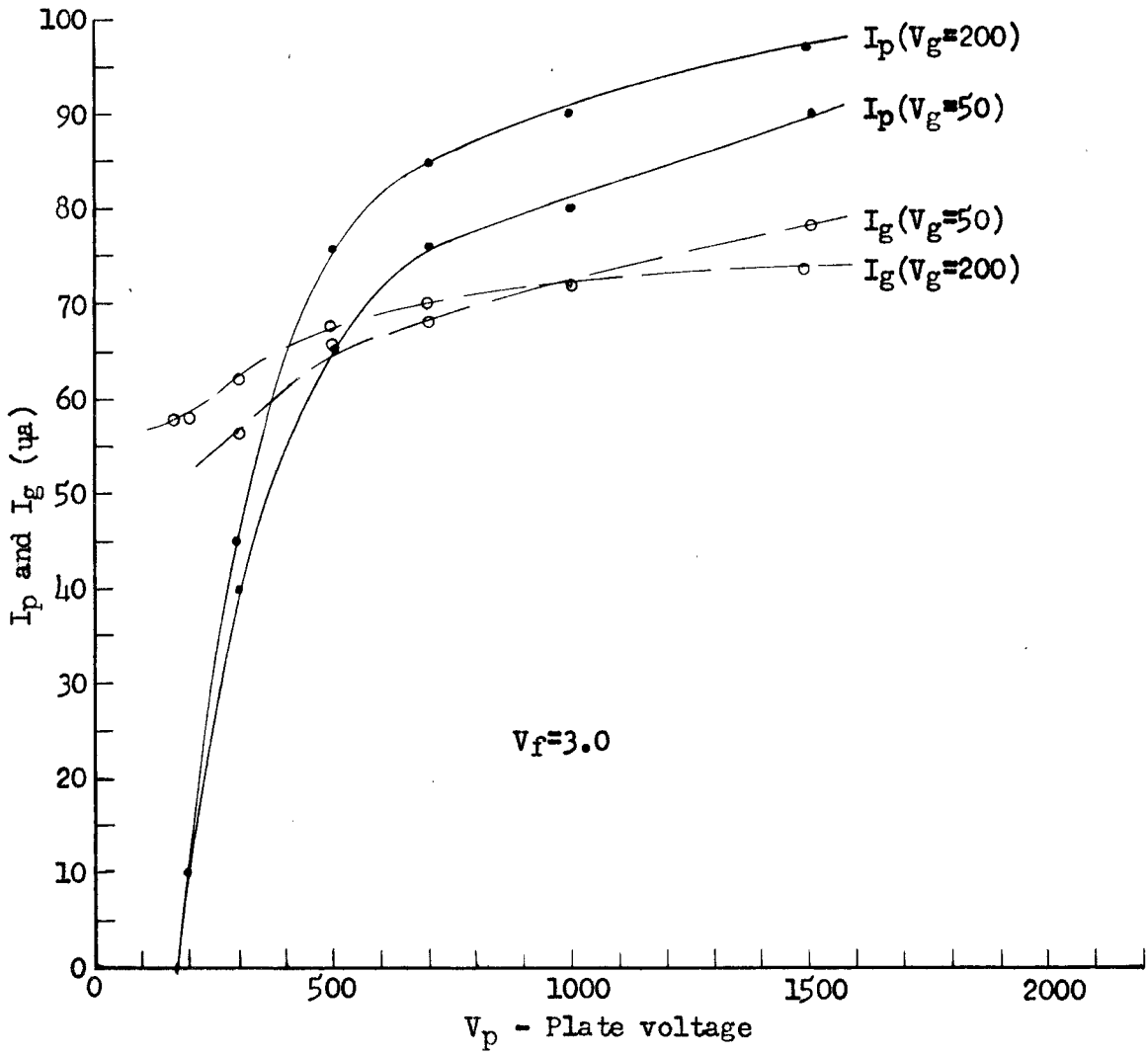

Figure 21. Plate characteristics of a triode device with a 0.05" disc of coarse-beaded ceramic between the grid and plate

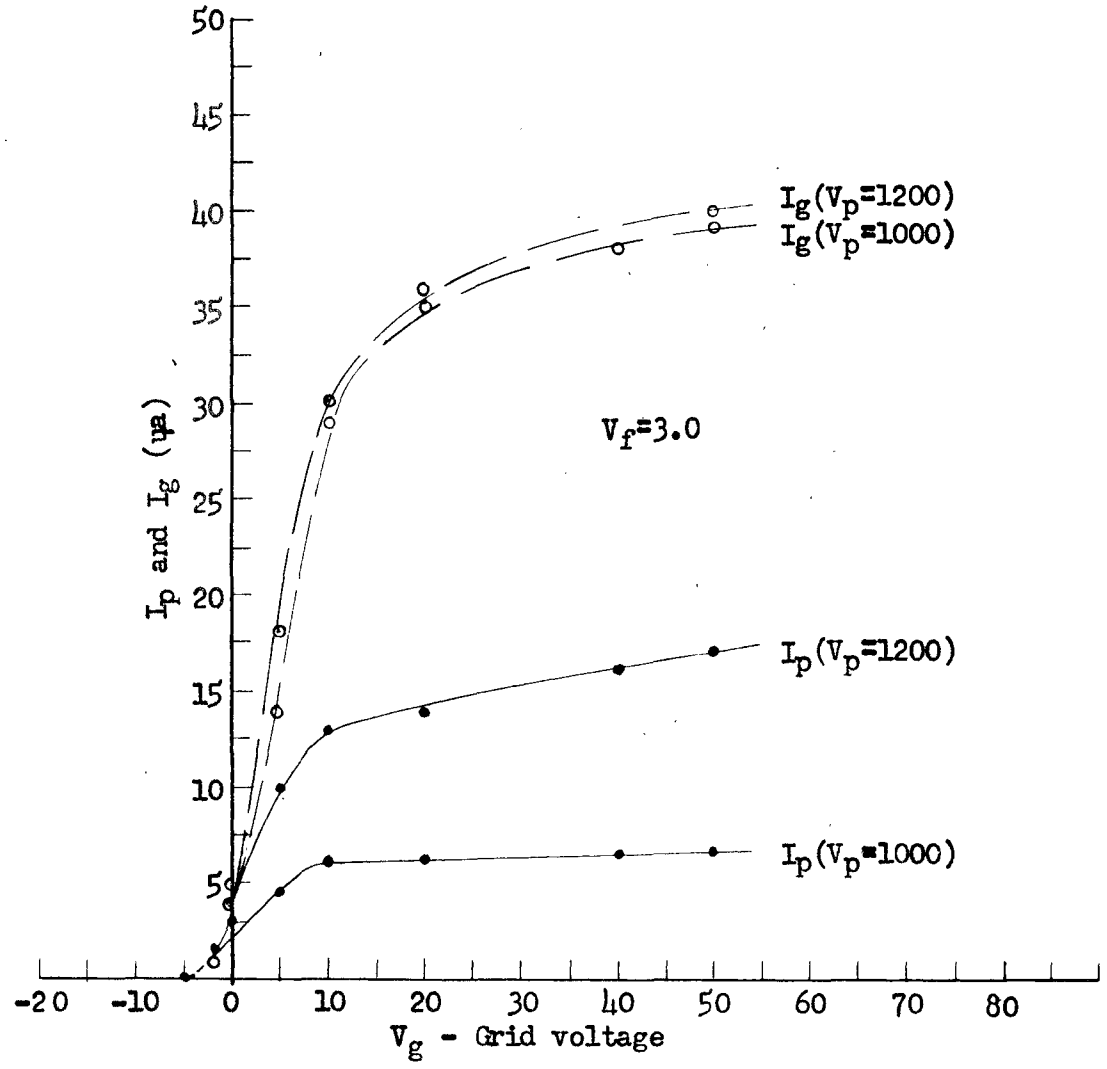

Figure 22. Grid characteristics of a triode device with a 0.07" disc of coarse-beaded ceramic between the grid and the plate

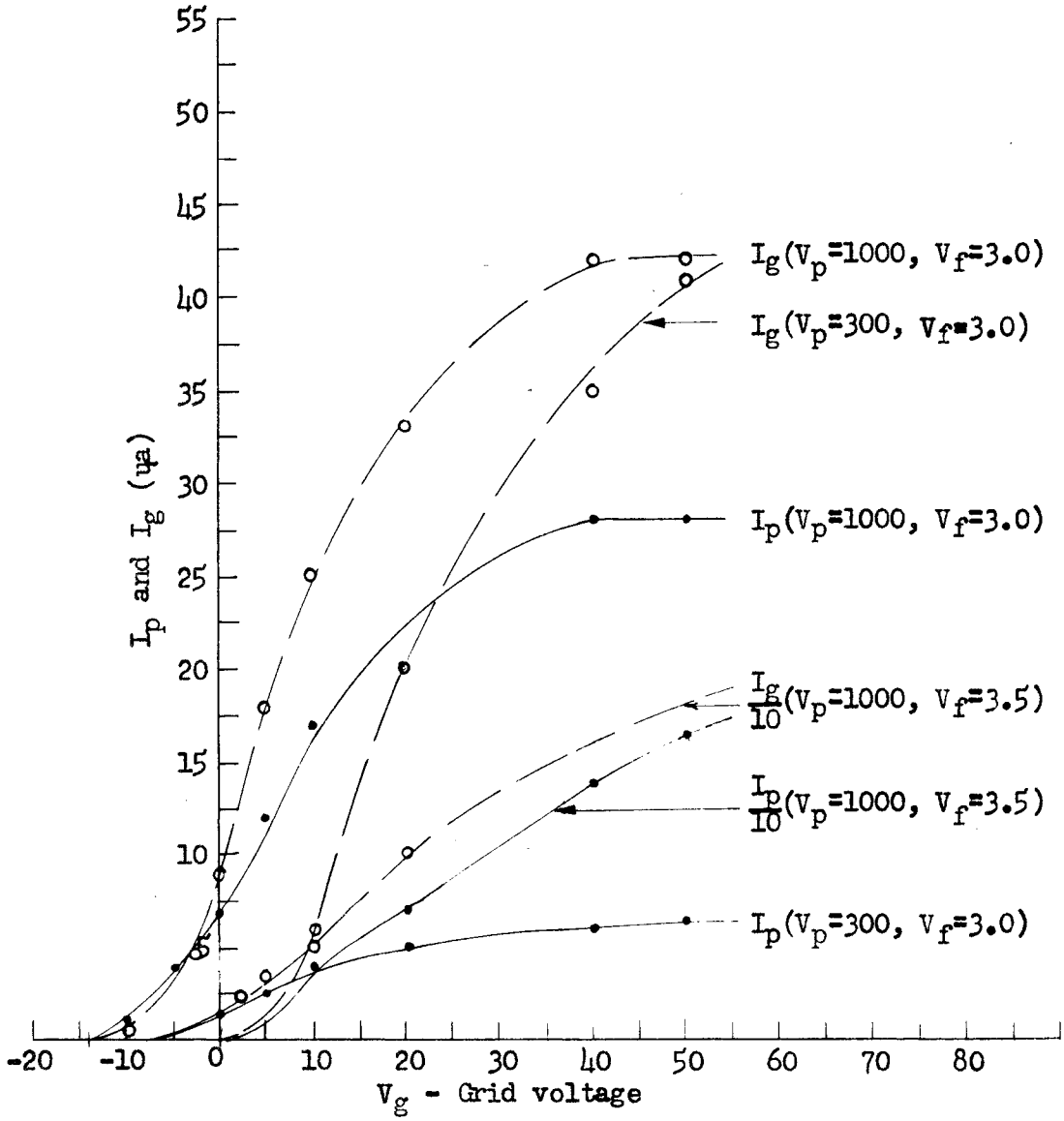

Figure 23. Grid characteristics of a triode device with a 0.05" disc of coarse-beaded ceramic between the grid and plate

Another result which adds to the general understanding of the electron behavior is that the spacing of the tungsten filament from the edge of the ceramic disc is not critical. Twenty per cent variation in the spacing gave no detectable change in the resulting current curves.

B. Analysis of Data

The data, as presented in the preceding section, establish the possibility of electron transfer through the pores of a ceramic spacer.

The nature of porous ceramics, in general, is such that a uniform system of pores is nonexistent. It is therefore difficult to present quantitative theoretical evidence of the same degree of reliability as that in the fields of semiconductors, electrolytic action, or ordered crystalline materials.

Early in this investigation the author did considerable research on the possibility of a dual conduction mechanism whereby electrons would progress simultaneously through both the structural and the open parts of a porous disc. Since a semiconductor is an insulator with various amounts of impurities, the recently developed theories of charged carriers in the solid-state are applicable to any structural conduction. Mott and Gurney (22) treat electronic processes in ionic crystals while electron mobility and semiconductor theories are discussed by Conwell (5) and others. With the following conclusions the conduction through the structural parts of the porous material is

eliminated from further consideration: (a) The electric fields and the temperature of the samples used in these tests were not sufficiently extreme to cause measurable conduction. This is evident from the test of the Norton disc, RA-98, which allowed no electronic transmission of any kind; (b) trapped electrons, whether trapped by closed pores or surface traps caused by crystal imperfections, reduce the conduction currents through structural parts to insignificance; (c) the theories used by Loosjes and Vink (21) to explain emission and re-emission from the pores of hot oxide coatings do not apply because of the much lower temperatures and higher work functions applicable in this investigation.

While conduction through the pore boundaries is negligible, the electron passage through the open pores is greatly affected by the shapes and nature of the pore boundaries. The irregularity of the pores makes an accurate theoretical derivation of the electron passage impossible. The random pores with their highly irregular boundaries offer a variety of obstacles to the electronic space-charge currents. Inelastic collisions of various degrees with such obstacles result in random scatterings which affect the final velocity and the transit time of the electrons. By far the greatest obstacle to electron passage is the space-charge-blocking of the small pores through which the electrons must pass. This action is highly exaggerated over that found in an ordinary vacuum tube because of the restricted and reduced areas. Qualitative consideration of these factors will follow a brief review of the well-established diode equations.

Throughout the derivations that follow the one-dimensional plane-electrode system is used. By spacing the spiral cathode at a distance from the plate greater than the separation of successive spiral turns, a simple flux plot shows the fields to be nearly plane in the region near the plate where the disc is located. While Poisson's equation in three dimensions applies to conditions at a point in the pore space, it is assumed that the volume element considered permits the use of the cathode-to-plate dimension only.

The following symbols are used to express the well known Child's law for the ideal vacuum diode using the m.k.s. rationalized system of units:

V_p - Plate to cathode voltage

E - Electric field intensity

d - Plate to cathode spacing

v - Velocity

J - Current density in amperes/m^2

V - Voltage of any point relative to the cathode

e - Magnitude of the electron charge (1.602×10^{-19} coulomb)

m - Mass of an electron (9.11×10^{-31} kg.)

ρ - Charge density (negative)

x - Variable distance from the cathode

ε - Dielectric constant of free space (8.85×10^{-12} farad/m).

The following column on the left lists the laws and boundary values used in the standard derivation of Child's equation, while the column on the right lists the various results of the complete derivation.

Equations and Assumptions	Results
$\frac{d^2V}{dx^2} = -\frac{\rho}{\varepsilon}$	$J = 2.33 \times 10^{-6} \frac{V_p^{3/2}}{d^2}$
$J = \rho v$	$V = k_1 x^{4/3}$
$Ve = 1/2\ mv^2$	$E = k_2 x^{1/3}$
v (at $x = 0$) $= 0$	$v = k_3 x^{2/3}$
E (field at $x = 0$) $= 0$	$\rho = k_4 x^{-2/3}$.

The results are also shown in graphical form in Figure 24. The shapes of these ideal diode curves are altered by the presence of the ceramic disc. The velocity curve is the most obviously affected since the electron collisions reduce the final velocity below that given by $v = \left(\frac{2eV_p}{m}\right)^{1/2}$.

The shapes of the ideal diode curves are also altered when a finite uniform emission velocity is assumed. The general result is that a space cloud of emitted electrons exists just outside the emitter forming a negative potential barrier which also acts as a velocity filter for other emitted electrons. Figure 25 shows, by comparison, the potential distribution resulting when initial electron velocities are considered. The minimum potential, V_m, and the location of the virtual cathode, x_m, are defined by Figure 25. The plate current density is then altered to be

$$J = 2.33 \times 10^{-6} \frac{(V_p - V_m)^{3/2}}{(d - x_m)^2}$$

where V_m has a negative value. A discussion of this equation is found in Spangenberg (31, p. 191). The magnitude of V_m is shown to be linearly

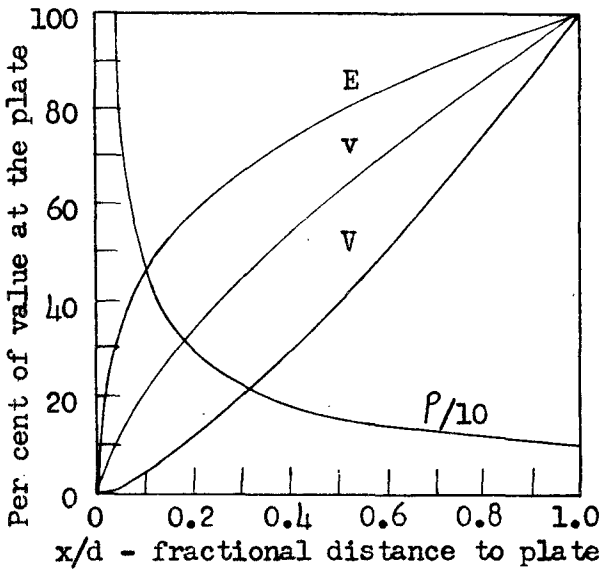

Figure 24. Ideal curves for space-charge-saturated diode between the cathode and plate. Electric field (E), electron velocity (v), potential (V), charge density (ρ)

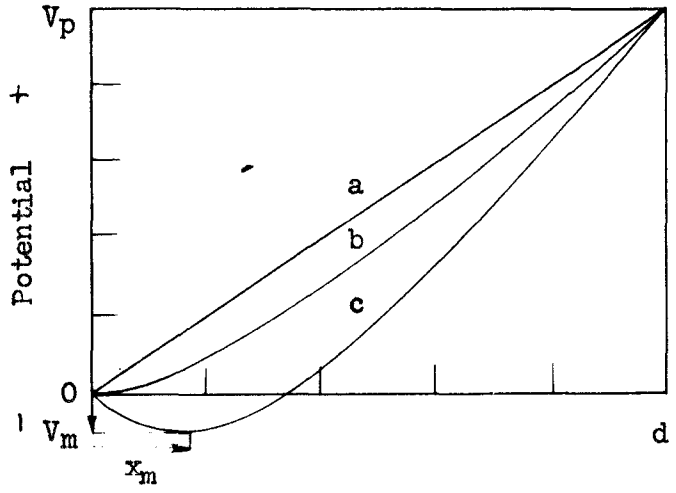

Figure 25. Potential distribution in a diode with (a) no space-charge, (b) space-charge limiting neglecting initial velocity, (c) space-charge limiting with initial velocity

related to the cathode temperature, while x_m depends upon the electrode spacing, the plate voltage and the value of V_m.

Still another detail that must be kept in mind when analyzing these data is the alteration of Child's law when a filamentary emitter is used. Spangenberg (31, p. 190) shows that the exponent of V_p varies from the usual value of 3/2 for V_p greater than V_f (filament voltage) to about 5/2 when V_p is smaller than V_f. This phenomenon is useful in triode theory and explains the large curvature of the plate characteristics near cut-off. The true exponent for a given electrode system can be determined only by a log-log plot of the experimental plate characteristics as is done later in this section.

Before proceding with the analysis of the plate characteristics, a study of electron velocities and the resulting effect upon the transmitted currents will be made. Figure 8 represents the reflector current vs the reflecting voltage as measured by the circuit of Figure 4 using a white fire-brick spacer. Figure 13 shows similar data for a coarse-beaded disc. Because the reflector potential (V_r) is necessarily less than the accelerating voltage of the plate (V_p), secondary electrons from the reflector are collected by the plate. When the curves of I_r go negative, secondary electrons exceed the primary electrons. The energy distribution can be obtained, if the primary reflector current (I_r') is known as a function of V_r, by

$$dI_r'/dV_r = df(V_r)/dV_r.$$

When the derivative on the right is plotted vs eV_r the resulting curve

represents the energy distribution of the electrons reaching the reflector. In other words, the slope of the I_r' vs V_r curve gives the energy distribution. If one further divides each ordinate of the dI_r'/dV_r curve by a constant that makes the area under the new curve unity, the ordinates of this new curve represents the probability that an electron will have the energy read on the abscissa scale. To illustrate, observe the assumed primary current (dotted curve) in the middle diagram of Figure 13 given by

$$I_r' = 0 \qquad V_r \leq 420$$

$$I_r' = 44(V_r - 420)/177\mu a \qquad 420 \leq V_r \leq 607$$

$$I_r' = 44\mu a \qquad 607 \leq V_r.$$

The energy distribution of the emitted electrons is Maxwellian and covers an energy range of about one to two electron volts, depending on the emitter operation. Because of the random scattering of the electrons going through the ceramic, the terminal energy range will be much wider. The minimum value of V_r (420 volts for the example chosen) is located as the point where the total reflector current is just measurable. The assumed primary reflector-current curve then rises linearly from that point to the value given when $V_r = V_p$ in two thirds of the remaining voltage interval. In this case the slope is 0 or constant at

$$\frac{dI_r'}{dV_r} = \frac{44}{177}.$$

The distribution is then rectangular and is centered about the average energy of 700 - 508.5 = 191.5 electron volts. Thus, under the

assumptions made here, the average electron arrives at the plate with a velocity of 8.2×10^6 m/sec compared to 15.15×10^6 m/sec with the ceramic absent. The average terminal velocity is reduced by a factor of 0.54. Using a similar method a reduction factor of 0.484 is found for the bottom curve where $V_p = 1000$ and 0.49 for the top diagram where $V_p = 500$. Considering Figure 8, one finds a velocity reduction factor of 0.795 for both curves. These results are reasonable since the coarse-beaded ceramic has a greater density of obstacles to the electron passage than does the white fire-brick.

The general effect of this velocity reduction is to decrease the plate current as indicated by $J = \rho v$ amperes/m^2. The actual relationship of velocity to the final current is more complicated as it is involved in the derivation of the current equation which follows. Assume an element of volume dxdydz so located that uniform parallel flux lines penetrate only the dydz surfaces and that the net charge movement and, therefore net space currents, have only x directed components as given by

$$J = \rho v. \tag{1}$$

From Gauss's law the net flux leaving is equal to the charge within the volume element or

$$D_x \Delta y \Delta z = \rho \Delta V = \rho \Delta x \Delta y \Delta z \tag{2}$$

where the flux density is $D_x = \varepsilon E_x$, called εE for simplicity. Equation (2) now reduces to the differential form

$$dE/dx = \rho/\varepsilon. \tag{3}$$

Substitute $E = -dV/dx$ and get

$$d^2V/dx^2 = -\rho/\varepsilon. \tag{4}$$

At this point the reduction of the kinetic energy by the presence of the ceramic disc enters as a velocity reduction factor represented by h, or

$$v = h(2eV/m)^{1/2}. \tag{5}$$

Substitution of equations (5) and (1) into (4) gives

$$d^2V/dx^2 = -(J/\varepsilon h)(m/2e)^{1/2}(V)^{-1/2}. \tag{6}$$

Obtain the exact differential by multiplying by dV/dx, integrate and obtain

$$(dV/dx)^2 = (-4J/\varepsilon h)(m/2e)^{1/2}(V)^{1/2} + C. \tag{7}$$

According to Figure 26 the electric field and the potential will be assumed 0 at $x = 0$. The constant of integration is therefore 0. By taking the square root of equation (7) and integrating, with the constant again 0, the potential distribution equation becomes

$$V = (-9J/4h\varepsilon)^{2/3}(m/2e)^{1/3}x^{4/3}. \tag{8}$$

Solving for the current density and evaluating the constants, where $V = V_p$ at $x = d$, gives

$$J = 2.33 \times 10^{-6}hV_p^{3/2}/d^2 \text{ amperes/area}. \tag{9}$$

This equation shows that the presence of the ceramic disc reduces the plate current and the terminal velocity of the electrons by the same factor h. According to Figure 26, if the electrons experience significant velocities in the region to the left of the chosen origin, the constants of integration in the preceding derivation are not zero, resulting in a more complicated solution.

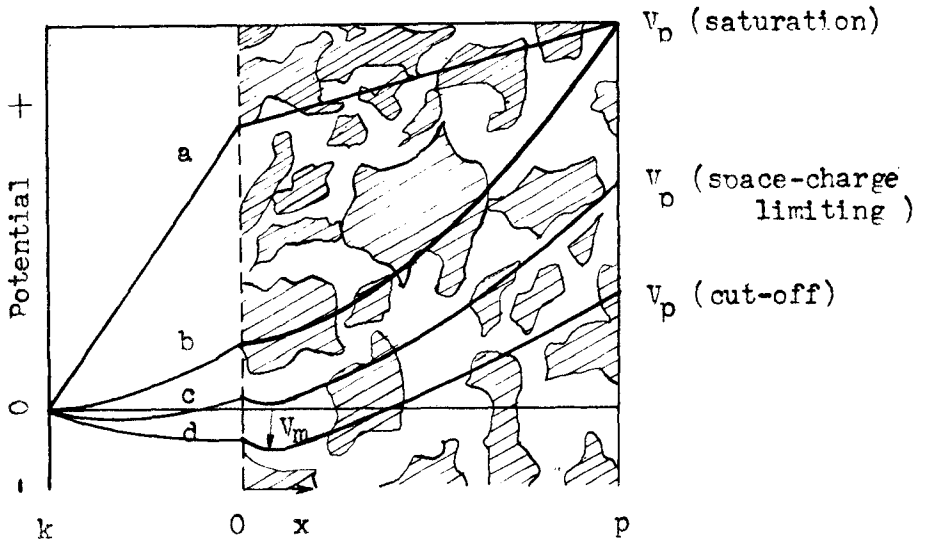

Figure 26. Sketch involving two-dimensional space; and postulated potential distributions in a diode device with a ceramic disc. (a) no space-charge, (b) space-charge with temperature limiting, (c) space-charge limiting, (d) cut-off

Continuing with the analysis, it is necessary to consider the plate characteristic curves of the diode device in three parts: At cut-off, where the curve is concave upward, and where the curve is concave downward. The curves of Figures 6, 9, 11, 14, and 17 illustrate the problem at hand. Also Figure 26 represents an estimate of the potential distribution within the diode device with a ceramic disc. The curves d, c, and b correspond respectively to the conditions of cut-off, space-charge limiting and temperature limiting. For example, as the plate

voltage, V_p is increased from the cut-off condition (curve d) the voltage distribution throughout the electrode space changes so that the average field intensity in both the void and the ceramic increases uniformly.

The apparent cut-off voltage is defined as the plate voltage that just prevents the flow of measurable plate current. The principal action involved is the blocking and repulsion of emitted electrons by the cloud of electrons that accumulates and becomes static in the space between the plate and the cathode. This space-cloud of electrons is greatly emphasized by the presence of the ceramic disc which causes a large reduction in the effective transmitting area. Also some electrons will become trapped by closed pores which offer a supplementary block of a quasi-permanent nature. The irregularities in the ceramic discs are evident in the microscopic pictures of Figure 1 and are estimated by an enlarged sketch in Figure 26. Such irregularity defies strict quantitative treatment. Using the subscript t for total quantities, an approximate mechanism is presented using n parallel transmission paths of different effective areas, where $A_t = \sum_{k=1}^{n} A_k$, and with random lengths ℓ_k. The total plate current is then written in the form

$$i_t = 2.33 \times 10^{-6} \, h \sum_{k=1}^{n} \frac{A_k V_p^{a_k}}{\ell_k^2} \qquad (10)$$

where A_k is highly variable while a_k and ℓ_k^2 are nearly constant.

As previously mentioned, cut-off is the result of space-charge-blocking of the pores. As depicted by Figure 26, there are two voltages that control the space currents in the ceramic filled device. The first is the plate voltage, V_p, which is established by an external power supply. The second voltage, V_m, is located near the inner edge of the ceramic disc and is often called the effective grid voltage in this dissertation. In that two voltages, V_p and V_m, are controlling the plate current, a device resembling a triode vacuum tube is present. The "grid" voltage in this case is not externally controlled but instead is a function of the plate voltage, increasing from negative to positive values as V_p increases.

Using this triode mechanism, cut-off is explained by the familiar triode arguments involving a quantity

$$I = K(V_m + V_p/w)^a. \tag{11}$$

As V_p decreases from a high positive value, V_m decreases from a positive value to a negative value as shown in Figure 26. This means at cut-off the positive V_p/w nullifies the negative V_m. The value of V_m at cut-off is given by the thermal energy as expressed in electron volts plus an effect from the non-equipotential filament. The contribution of the plate voltage, when referred to the location of the potential minimum, is given as V_p/w where w is obviously proportional to the ceramic density and thickness, and inversely proportional to the "electron permeability". Thus w is very similar to the amplification factor μ of a triode, which measures effectiveness of the grid voltage compared to

plate voltage in controlling the plate current. The values of w, as calculated from the cut-off conditions are given in Table 1 for the ceramic samples tested.

With an assumed value of $V_m = -4.7$ at cut-off, a sample calculation of the cut-off factor, using the 0.05 inch fire-brick disc and $V_f = 3$ (see Figure 6), gives $w = -V_p/V_m = -80/-4.7 = 17.0$. Similarly for the less permeable 0.052 inch coarse-beaded disc, $w = -350/-4.7 = 74.5$.

Considering the concave upward portion of the plate curves, it is necessary to employ both the effective area equation (10) and the triode equation (11).

The triode equation, as applied here, differs from the ordinary vacuum tube application in that V_m is dependent upon V_p as shown by curve c of Figure 26. Thus as V_p/w increases, V_m goes from the negative cut-off value through zero to positive values. This means qualitatively that both terms act to increase the current according to an exponent of V_p which is greater than the theoretical 3/2 or 5/2 as the case may be.

The other consideration which also causes a rapid rise in the plate current as V_p is increased involves the multiple areas of transmission (see equation 10). Consider an area which is large compared to a nearby small area of transmission. The large area will start to conduct first as the plate voltage is increased. However, in so doing the space charge which creates the stopping voltage, V_m, at the entrance of the smaller area is decreased. This, in turn, opens the smaller area to conduction; and the spreading continues as a "cumulative area" action as V_p increases.

Table 1

Summary of diode data analysis

Disc material	Thickness (inches)	Porosity factor	Filament voltage (V_f) (volts)	Cut-off plate voltage (volts)	Cut-off factor $w = -V_f/V_m$	Plate voltage exponent (a)
White fire-brick	0.050	0.515	3.5	80	17.0	2.4
	0.050	0.515	3.0	80	17.0	2.7
	0.070	0.515	3.5	100	21.3	2.6
	0.070	0.515	3.0	100	21.3	2.9
Ceramic gasoline filter	0.070	0.830	3.5	350	74.5	7.4
	0.070	0.830	3.0	350	74.5	7.5
	0.080	0.830	3.5	500	106	7.4
	0.080	0.830	3.0	500	106	7.8
Coarse-beaded A SiMag 576	0.050	0.564	3.5	350	74.5	6.6
	0.050	0.564	3.0	350	74.5	6.7
	0.070	0.564	3.5	600	127	10.8
	0.070	0.564	3.0	600	127	11.0
Fine-beaded A SiMag 576	0.050	0.594	3.5	875	186	14.0
	0.070	0.594	3.5	1270	270	15.2
Crucible sieve	0.062	0.900	3.5	120	25.5	2.6
	0.075	0.900	3.5	150	32.0	2.8
Norton ceramic RA-98	0.050	0.980	3.5	No current transmission occurred		

While in the space-charge-controlled region, both of the mechanisms just described cause the transmission current to increase as an exponential power of the plate voltage. The combined effects result in a plate current given by

$$i = K V_p^a \qquad (13)$$

where K is a constant and "a" is evaluated from the slope of the log-log plot of i vs V_p. The calculated values of "a" are given in Table 1.

The above mechanisms are substantiated by the tests made on the Coors crucible with uniform holes. From Figures 17 and 18, using $V_f = 3.5$, values of "a" are found to be 2.6 and 2.8 for thickness of 0.062 inch and 0.075 inch respectively. The "cumulative area" theory contributes little to this case where areas are equal and conduct simultaneously. An "a" of 14 for the 0.05 inch coarse-beaded disc (see Figure 16), where the transmission areas are irregular, illustrates the cumulative conduction.

The concave downward part of the plate characteristics is explained by various degrees of saturation. Many elementary textbooks picture a very sharp and definite break in the curve where space-charge limiting stops and temperature limiting or temperature saturation starts. In all practical devices the transfer is gradual since the cool ends of the emitter start the temperature limiting action at a lower voltage than is required to saturate the hotter portions. This action coupled with the multiple areas that may approach saturation differently, accounts for the transition. From the curves it is obvious that those with the low

filament voltage saturate quickly at low values of plate current.

Besides producing higher values of temperature-limited currents, higher filament voltages cause changes in the space-charge-controlled regions of the plate characteristics. Figures 11, 14, and 17 show these effects of increased emission when the filament voltage is raised from 3.0 to 3.5 volts. Figure 16 shows an enlarged plot of this phenomenon where the curves of the two filament voltages cross. The high filament voltage, $V_f = 3.5$, presents a more dense cloud and therefore a greater blocking action than does the filament voltage of 3.0 in the region near cut-off. Another demonstration of the same principle is found in Figure 17; where data on a 0.062 inch crucible sieve are shown over a wide range of voltages so that the saturation effects are obvious. Each curve is normalized to the current at 1000 volts, which allows close comparison of the curve shapes.

Figure 18, in addition to illustrating the theory of the preceding paragraph, compares directly the corresponding curves with and without the ceramic disc present. An interesting and an important conclusion is that the presence of the disc causes a delay or a shift in the curves to higher voltages. The temperature saturation effects are similar at nearly equal current levels.

Before getting into the analysis of the triode data, it is necessary to review the circuit used in making the measurements as shown in Figure 5. Notice particularly that the plate voltage V_p is still the voltage across the ceramic sample and is measured from the grid. The plate and grid currents are metered separately so that the total

cathode current is obtained as their sum.

Figure 19 is a study of current division between the positive grid and the plate, in the absence of a ceramic disc. Once saturation is reached the plate voltage has little effect upon either the plate or grid currents. Figures 20 and 21 are interesting studies in plate characteristics with a ceramic disc at different values of constant V_g and V_f. The division of grid and plate current is evident in all cases but is not important to this analysis.

The three parts of the plate characteristics (cut-off, space-charge limiting, and saturation) are evident and correspond to the theories just presented. Again there is cut-off in the plate circuit even though the electrons have from 10 to 200 electron-volts of "initial energy" upon arrival at the ceramic surface. The initial energy of the electrons does lower the cut-off voltage from 350 to 175 for the 0.052 inch disc of coarse beads and from 600 to 300 for the 0.07 inch disc. The coarse-beaded material, with its many areas of transmission, diffuses the electron beam; and the space cloud again causes cut-off. Less potential difference is now required, however, to start the conduction with the aid of the initial energies. The grid characteristics of Figures 22 and 23 are self explanatory and offer studies primarily of saturation effects. The curves show that the higher plate voltages require the more negative grid voltages for cut-off; which substantiates the previous triode theory of cut-off.

IV. DISCUSSION

A. Factors Affecting Electron Passage Through Pores

The estimated size of an electron as a particle, 1.9×10^{-13} cm in radius, is many orders of magnitude smaller than the pores in a ceramic or even the lattice spacings of the crystals. Therefore, the particle size offers no physical restriction to electron movement. Instead, the electron is controlled by forces which result from the electron's charge and the fields surrounding it. Because of the concentration of fields and forces in the structure of an insulating solid, electron motion in or through it is negligibly small at ordinary operating temperatures. In porous ceramics, electron passage through the openings or pore space is also restricted, primarily by the repelling fields of other electrons. This action, called space-charge-limiting, is present in the pores and reduces the electron current. Even though an external potential is applied, the free electrons reshape the internal fields and represent the basic control. Many things, however, affect the space-charge density.

The shapes and sizes of the pores are most important in this study. The density by weight is not an effective measure of a material's permeability to electron flow. More important is the density of open pores that do not trap or block the electron's progress to the attracting

electrode. A ceramic is highly permeable to electrons if it has a high density of pores with large effective areas, and if the electron paths are short and extend through the sample. The samples described and used in the experimental part of this thesis represent a variety of these controlling factors. For example, the white fire-brick and the gasoline filter had highly uneven pores with a wide range of areas and short lengths with many closed pores. In contrast, the sintered spheres making up the coarse-beaded discs had small but somewhat uniform areas. The electron paths were lengthened by the random placement of the spheres but the majority of the pores were open. A third type is represented by the crucible discs with a few holes of uniform areas and with minimum lengths.

The voltage delay, represented by the shifting of the cut-off point from the origin to a positive plate voltage, is controlled by the factors discussed in the previous paragraph. In general the amount of shift or delay is proportional to the volume density, the effective path lengths and the number of traps; while it is inversely proportional to the porosity factor, the size and number of the areas.

As shown by the curves, the sharpness of the saturation effect is also governed by these factors. The unobstructed holes of the crucible sieve cause a fairly quick and definite saturation, while other samples with restricted paths have a gradual transfer from the space-charge region to the temperature-limited region.

B. Possible Applications

As mentioned in the introduction, one of the most difficult problems in the reliable tube program is that of spacing and holding the elements. Under shock and vibration the tube elements may shift and may cause a change in the tube characteristics or complete failure. By using highly opened and permeable ceramic spacers, through which electrons could pass, the electrodes could be rigidly embedded and held. It is possible that the elements could be sandwiched between ceramic layers or, if made of a sufficiently refractory metal, the electrodes might be included when the ceramic is fired.

While considering possible applications, it must be remembered that no ceramic materials have been manufactured with this application in mind. The samples available for this experiment do not, therefore, represent an accurate prediction of the ultimate capabilities of such devices. By controlling pore shapes and density, an unlimited variety of operating characteristics could be obtained. Both linear and non-linear characteristics could result in applications to analogue devices, control circuits, counting devices, function generators and others. The delayed cut-off characteristic could be used in overload protection or regulating apparatus.

The introduction of a gas into the ceramic device would certainly produce some interesting and perhaps practical results. The space-charge that limits the passage of electrons could be neutralized by the

ionized gas according to the same action that allows the high currents through hot-cathode gas rectifier tubes. Such neutralization within the pore space of a diode device would establish the same high currents that exist in the present gas diode. An advantage would then be obtained if a grid could be embedded in the porous ceramic, and situated so that the ordinary positive-ion blocking of the grid is prevented. This would allow for a gas tube to retain complete control of the conduction current. By carrying the above reasoning a step further it may be possible to eliminate the filamentary cathode emitter. Such a cathode might consist of two closely spaced electrode points in a small gas-filled volume. The ceramic of a proper porosity would surround the ionizing chamber and contain the remaining electrodes. It is conceivable that the ionization would remain mostly within the chamber while the electrons of the ionization process could be transmitted through the pores. Thus the troublesome filamentary cathode might be replaced with a steady gas discharge in high current applications where the "noise" of the discharge could be tolerated.

Still another area of possible application of electron passage through porous ceramics is an extension of the ceramic tube envelope described by Palmer (26). His article describes a ceramic envelope which is glazed on the outside, and replaces the metal or glass envelope now used. Perhaps a porous ceramic could be used for the inner part to hold the elements and leads; while the outer pores could be filled and glazed until vacuum tight. Such a device in cylindrical or spherical shape might be extremely compact and rugged.

C. Future Investigations

In an initial investigation such as this, many possibilities of further research become apparent. For example, the possible applications mentioned in the preceding section are unknown and offer possibilities for future investigation. Those possibilities are not repeated here, but general methods of attack are discussed.

The success of the research represented by this thesis opens up another possibility of fundamental investigation, namely, the effect of gas ionization in the passage of electrons through porous ceramics. Such research can be performed in ordinary laboratories. The construction of the experimental apparatus would necessarily require provisions for sealing off the vacuum chamber and then leaking in a measured quantity of an inert gas such as argon. Simple calculations would give the resulting pressure under controlled temperature conditions. Electron conduction could then be measured as a function of many variables.

Many projects leading to practical applications are possible. However, in these cases it is imperative that close cooperation with a ceramic laboratory and with a laboratory familiar with vacuum tube construction be available. Actual assembled products could then be constructed and sealed off for testing under typical operating conditions. It is certain that ceramic engineers, familiar with techniques of refractories, could make to order a variety of porous materials for

testing. The idea of the sintered beads should be continued. It is conceivable that "artificial" pores could be punched or drilled before baking, so that very great transmission areas would be present and the ceramic would still have sufficient strength to support the electrodes in a firm manner.

V. SUMMARY

Ceramic discs, if sufficiently porous, are permeable to free electrons under the influence of an electric field. Plate characteristics, taken from tests on a diode circuit, exhibit curves that consist of three important parts: Cut-off or the voltage at which plate current is just measurable, the concave upward or space-charge-limited part, and the concave downward portion where temperature saturation is apparent. The controlling factor in the first two cases is the space-charge that exists near the cathode side of the porous disc. At high plate voltages the saturation becomes complete as all the emitted electrons are transferred directly to the plate; which means the limiting electron cloud is dissolved.

More specifically the conditions at cut-off are caused by the electron cloud which creates a negative potential sheath, V_m, at the cathode side of the disc. By using the triode analogy, the effectiveness of the plate voltage is reduced by the constant w so that the plate current is given by

$$I = K(V_m + V_p/w)^a. \tag{11}$$

Here, V_m is not independent of V_p and increases from negative to positive values as V_p increases. Cut-off occurs when the negative V_m is equal in magnitude to V_p/w.

As V_p rises above the cut-off value the plate current rises as an exponential function of V_p. The exponent in this case is greater than that predicted by the Child-Langmuir space-charge equations of an ordinary vacuum tube. The highly random pore shapes which offer transmission paths having a variety of areas (A_k) and lengths (ℓ_k) defy accurate quantitative derivations. A qualitative treatment uses n parallel transmission paths where the total current is given by

$$i_t = 2.33 \times 10^{-6} \, h \sum_{k=1}^{n} \frac{A_k V_p^{a_k}}{\ell_k^2} \qquad (10)$$

where h is the electron velocity reduction factor caused by inelastic collisions. In this equation a_k and ℓ_k are nearly constant for a given sample but the areas, A_k, are highly variable. As the plate voltage V_p increases, the larger areas conduct first. Such conduction decreases the density of the blocking electron sheath and conduction spreads to smaller areas in a cumulative action. This increasing area and the changing V_m, both being a function of V_p, result in the space-charge-limiting diode equation

$$i = K V_p^{a}. \qquad (13)$$

The value of "a" is obtained as the slope of the log-log plot of i vs V_p, and was found to vary from 2.4 to 15.2 for the samples tested.

When the electrons are given initial velocities by making the grid of a triode device positive, the cut-off potential is reduced. The electrons divide between the grid and the plate. At low plate voltages, the electrons that enter the restricted ceramic-filled region between

the grid and the plate lose their initial energies and establish the blocking sheath of electrons. The shape of the triode plate characteristics are similar to those of the corresponding diodes except for the reduced cut-off voltages.

Some of the factors affecting the transmission of electrons through porous ceramic discs are: The length of the electron path, the number and size of the transmitting areas, and the density of the closed pores or electron traps. The density by weight of the porous ceramic is not an effective measure of its permeability to electron flow. More important is the density of open pores that do not trap or block the electron's progress to the attracting electrode.

For purposes of application, the porosity of the ceramic material need not come from the loose packing or from the firing of included organic materials. Deliberate designs such as cylindrical or conical holes are possible if formed before the ceramic is fired. Such a procedure would retain the desirable mechanical strength and support, and improve the permeability. By including an appropriate gas in the device the resulting ionization and space-charge neutralization could enhance the electron flow through porous media.

VI. SELECTED REFERENCES

1. Acheson, M. A. and McElwee, E. M. Concerning the reliability of electron tubes. Proc. I.R.E. 40: 1204-1206. 1952.

2. Barrer, R. M. The measurement of surface area of finely divided solids by the flow of gases through them. British J. Appl. Phys. Supp. No. 3. S41-S47. 1954.

3. Chaffee, E. L. The characteristic curves of the triode. Proc. I.R.E. 30: 383-395. 1942.

4. Coblenz, A. and Owens, H. L. Physical properties of electrons in solids. Electronics. 26: 162-165. May 1953.

5. Conwell, Esther M. Properties of silicon and germanium. Proc. I.R.E. 40: 1327-1337. 1952.

6. Deb, S. Current division in plane positive grid triode. Indian J. Phys. 26: 377-392. Aug. 1952.

7. Dow, William G. Fundamentals of engineering electronics. 2nd ed. N. Y. John Wiley and Sons, Inc. 1952.

8. Dumond, T. C. Engineering materials manual. N. Y. Reinhold Publishing Corp. 1951.

9. Dushman, S. Vacuum technique. N. Y. John Wiley and Sons, Inc. 1949.

10. Forman, R. Measurement and theoretical study of electrical conductivity and Hall effect in oxide cathodes. Phys. Rev. 96, pt. 2: 1479-1486. 1954.

11. Frolich, H. Theory of dielectrics. Oxford. Clarendon Press. 1949.

12. Hahn, W. C. Effects of hydrostatic pressure on electron flow in diodes. Proc. I.R.E. 36: 1115-1121. 1948.

13. Hensley, E. B. On the electrical properties of porous semiconductors. J. Appl. Phys. 23, pt. 2: 1122-1129. 1952.

14. Hill, D. R. New cathode design improves tube reliability. Electronics. 24: 104-106. Aug. 1951.

15. Ijdens, R. A. Ceramics and their manufacture. Philips Tech. Rev. 10: 205-213. July 1948 - June 1949.

16. Jaffe, George. On the currents carried by electrons of uniform initial velocity. Phys. Rev. 65, pt. 2: 91-98. 1944.

17. Jost, W. Diffusion in solids, liquids, gases. N. Y. Academic Press, Inc. 1952.

18. Kohl, W. H. Materials technology for electron tubes. N. Y. Reinhold Publishing Corp. 1951.

19. Lafferty, J. M. Boride cathodes. J. Appl. Phys. 22, No. 3: 299-309. 1951.

20. Lindsay, E. W. and Berberich, L. J. Electrical properties of ceramics. Elec. Eng. 67: 440. 1948.

21. Loosjes, R. and Vink, H. J. The conduction mechanism in oxide-coated cathodes. Philips Res. Repts. 4: 449-475. 1949.

22. Mott, N. F. and Gurney, R. W. Electronic processes in ionic crystals. Oxford. Clarendon Press. 1940.

23. Muskat, M. The flow of homogeneous fluids through porous media. N. Y. McGraw-Hill Book Co., Inc. 1937.

24. Navias, L. Advances in ceramics related to electronic tube developments. J. Amer. Ceram. Soc. 37: 329-350. 1954.

25. Newcomb, R. Ceramic whitewares. N. Y. Pitman Publishing Corp. 1947.

26. Palmer, Robert N. Ceramic tube mount for automatic assembly. Electronics. 27: 162-165. Aug. 1954.

27. Poritsky, H. Electron-gas equations for electron flow in diodes. Trans. Prof. Group of Electron Devices, I.R.E. p. 60-84. Jan. 1953.

28. Rose, A. R.C.A. Princeton, N. J. Information on space-charge currents in thin insulators. [Private communication.] 1954.

29. Shindo, T. Space-charge effects in the oxide-cathode layer. J. Phys. Soc. Japan. 8, pt. 2: 494-499. 1953.

30. Spangenberg, K. R. Current division in plane-electrode triodes. Proc. I.R.E. 28: 226-236. 1940.

31. _____. Vacuum tubes. N. Y. McGraw-Hill Book Co., Inc. 1942.

32. Strong, J. Procedures in experimental physics. N. Y. Prentice-Hall, Inc. 1941.

33. Tomlinson, T. B. On the conductivity of oxide cathode coatings. J. Appl. Phys. 25, pt. 1: 720-724. 1954.

34. Torkar, K. Property relationship of porous material. Ber. Deut. Keram. Ges. 31: 148-156. 1954.

35. Whitehead, S. Dielectric breakdown of solids. Oxford. Clarendon Press. 1951.

36. Wright, D. A. and Woods, J. The emission from oxide-coated cathodes in an accelerating field. Proc. Phys. Soc. London. 65, sec. B: 134-148. 1952.

VII. ACKNOWLEDGMENTS

The author wishes to express his appreciation to Professor W. L. Cassell for his encouragement and helpful criticisms; to Dr. George R. Town of the Engineering Experiment Station for the aid afforded; and to the staff members of the Electrical Engineering Department who assisted in many ways. Appreciation is also extended to my former student, Ferd Mullersman of the General Electric Tube Works at Owensboro, Kentucky, for assistance with the oxide cathodes; and to Dr. Hans Thurnauer and J. W. Deaderick of the American Lava Research Laboratory for their interest and help in supplying ceramic samples.